**CHARLES UNIVERSITY**

**FACULTY OF PHARMACY IN HRADEC KRÁLOVÉ**



DIPLOMA THESIS

# SYNTHESIS OF PROTEIN-KINASE INHIBITORS AS A POTENTIAL TREATMENT FOR CANCER

SARA MERDITA

Supervisor: Assoc. Prof. PharmDr. Jaroslav Roh, PhD.

Advisors: PharmDr. Lukáš Górecki, PhD.;

Assoc. Prof. PharmDr. Jan Korábečný, PhD.

HRADEC KRÁLOVÉ                                    2022

## DECLARATION

*Hereby I declare that this thesis is my own work. All literature and sources of information I used are listed in references and they are properly cited. This work has not been used to gain equal or different degree.*

HRADEC KRÁLOVÉ 2022                                                    SARA MERDITA

# TABLE OF CONTENTS

# LIST OF ABBREVIATIONS

APE1 – apurinic/apyrimidinic endonuclease 1

ATM – ataxia telangiectasia mutated

ATR- ataxia telangiectasia mutated and Rad3 related

ATRi – ataxia telangiectasia mutated and Rad3 related kinase inhibitor

ATRIP - ATR interacting protein

BER – base excision repair

*BRCA1/2* – breast cancer (genes) 1/2

CDC25A – cell division cycle 25A (phosphatase)

CDDP - cisplatin

CDK – cyclin-dependent kinase

*CDKN2A* – cyclin-dependent kinase inhibitor 2A

CSA/CSB - Cockayne syndrome group A/B protein

CT – computed tomography

DDR – DNA damage response

DNA-PKcs – DNA-dependent protein kinase

DSBs- double strand breaks

ERCC1- excision repair cross-complementing protein 1

ETAA1 – Ewing tumor-associated antigen 1

EXO1 – exonuclease 1

FANCI – Fanconi anemia group 1

FN HK – Fakultní nemocnice v Hradci Králové

GBM - glioblastoma

HPV – human papillomavirus

HR – homologous recombination

ICD-10 – International Classification of Diseases – Tenth Revision

*KRAS* - Kirsten rat sarcoma virus (gene)

Lig I/IV – DNA ligase I/IV

MCM – minichromosome maintenance complex

MGMT - $O^6$-methylguanine methyltransferase

MMR – mismatch repair

MRN - MRE11-RAD50-NBS1 (complex)

MRN – MRE11-RAD50-NBS1 complex

mTOR – mammalian target of rapamycin

NER – nucleotide excision repair

NHEJ – non-homologous end joining

NOR – Národní onkologický registr

PARG – poly(ADP-ribose) glycohydrolase

PARP - poly(ADP-ribose) polymerase

PARPi - poly(ADP-ribose) polymerase inhibitor

PCNA – proliferating cell nuclear antigen

PI3K – phosphatidylinositol 3-kinases

PIKK - phosphatidylinositol 3-kinase related kinases

PNKP – polynucleotide kinase-phosphatase

Pol $\delta$ - DNA polymerase delta

Pol$\beta$ - DNA polymerase beta

RFC – replication factor C

RHINO - RAD9-RAD1-HUS-interacting nuclear orphan

RNA pol2 - RNA polymerase II

ROS – reactive oxygen species

RPA – replication protein A

*RRM2* - ribonucleotide reductase regulatory subunit M2

SCLC – small-cell lung cancer

SMARCAL1 – SWI/SWF-related matrix-associated actin-dependent regulator of chromatin subfamily A-like protein 1

SSB- single strand break

TFIIH – transcription factor II H

TME – tumor microenvironment

TMZ - temozolomide

TOPB1 - topoisomerase II binding protein 1

UH HK – University Hospital in Hradec Králové

WRN – Werner syndrome helicase

XLF – XRCC-like factor

XPC C/F/G - Xeroderma pigmentosum complementation group C/F/G

XRCC 1/4 – X-ray repair cross complementing protein 1/4

# ABSTRAKT

Univerzita Karlova

Farmaceutická fakulta v Hradci Králové

Katedra organické a bioorganické chemie

ve spolupráci s Centrem biomedicinského výzkumu FN HK


**Autorka**: Sara Merdita

**Školitel**: doc. PharmDr. Jaroslav Roh, PhD.

**Konzultanti**: PharmDr. Lukáš Górecki, PhD.; doc. PharmDr. Jan Korábečný, PhD.

**Název diplomové práce:** Syntéza inhibitorů proteinových kináz využitelných v terapii nádorových onemocnění

Zhoubné nádory jsou jednou z hlavních příčin úmrtí po celém světě, což motivuje výzkumníky vyvinout léčbu, která selektivně cílí na nádorové buňky a zároveň ušetří zdravé buňky. Hlavní celkovou strategií je využít rysy specifické pro nádory. Ty jsou reprezentovány například nestabilitou genomové integrity a narušenou schopností opravy poškozené DNA (anglicky DDR). DDR se skládá z kaskád kináz a dalších proteinů a poslů, z nichž jsme se soustředili na syntetickou letální interakci mezi kinázami ATM (ataxia-telangiectasia mutated) a ATR (ATM and Rad3 related). Tyto dvě kinázy jsou předními hnacími silami v DDR, kde u nádorů má ATM tendenci být mutována, tedy dysfunkční, a tudíž životaschopnost buněk zbývá na ATR. Inhibice ATR je z toho důvodu zvláště atraktivní strategií pro eliminaci nádorových buněk, aniž by přitom byly zasaženy buňky zdravé. Čtyři inhibitory ATR již vstoupily do klinických studií jako protinádorové látky – VX-970, VX-803, BAY1895344 a AZD6738. Na základě jejich společných strukturních vlastností a několika specifik, především kandidátního léčiva VX-870 a jeho vývojového prekurzoru VE-821, jsme navrhli a připravili 15 nových molekul založených na 7-azaindolovém a 2,7-diazaindolovém jádru. Jejich cytotoxicita byla stanovena proti devíti rakovinným a jedné zdravé buněčné linii, kdy v monoterapeutickém režimu několik sloučenin vykázalo významnou inhibici proliferace nádorových buněk včetně buněčné linie primárního glioblastomu. Aktivita u kombinačního režimu s cisplatinou nebo temozolomidem byla především aditivního charakteru.

# ABSTRACT

Charles University

Faculty of Pharmacy in Hradec Králové

Department of Organic and Bioorganic Chemistry

in collaboration with Biomedical Research Center UH HK


**Author**: Sara Merdita

**Supervisor**: Assoc. Prof. PharmD. Jaroslav Roh, PhD.

**Advisors**: PharmD. Lukáš Górecki, PhD.;

                   Assoc. Prof. PharmD. Jan Korábečný, PhD.

**Title of diploma thesis**: Synthesis of protein-kinase inhibitors as a potential treatment for cancer

Cancer is one of the leading causes of fatalities worldwide, which is attracting attention of many researchers with desire to develop treatments that selectively target cancerous cells while simultaneously sparing healthy cells. The main overall strategy is to exploit features specific to cancer – the cancer hallmarks. Those are represented, for instance, by genomic instability and aberrant DNA damage response (DDR) pathways. The DDR consists of cascades of kinases and other proteins and messengers, where we highlighted the synthetic lethal interaction between the kinases ATM (ataxia-telangiectasia mutated) and ATR (ATM and Rad3-related). The two are major driving forces in the DDR, where in cancer ATM tends to be mutated and therefore dysfunctional, making the cells' viability reliant on ATR. Thus, ATR inhibition makes a particularly attractive strategy for abrogating cancer survival without affecting the healthy cells. Four ATR inhibitors have already entered clinical trials as anticancer agents - VX-970, VX-803, BAY1895344 and AZD6738. Based on their common structural features and several specificities, with particular focus on VX-970 and its developmental precursor VE-821, we have designed and synthesized 15 novel molecules built on 7-azaindole and 2,7-diazaindole core strucures. These were screened for cytotoxicity against nine cancer and one healthy cell line, with several compounds showing a significant inhibition of cancer cell proliferation in single-agent mode. Combinatorial regimen with cisplatin or temozolomide showed only moderate efficacy with an additive effect.

# 1 INTRODUCTION

## 1.1 Cancer

Neoplasm is classified as an abnormal mass of tissue, the growth of which is uncontrolled.[1] Therefore, neoplasms are composed of living cells which differ from the cells of the normal organ by the mutations causing the control of cell division, death, and differentiation to be lost at several different degrees. As a result, cells may appear different or even acquire new functions such as invasion and metastasis. According to these criteria, we can divide neoplasms into two main categories: benign tumors and malignant neoplasms.

Benign tumors do not have the ability of invading the surrounding or, for that matter, distant tissues, thus their growth is not life threatening as their clinical course is predictable.[1] Although they may cause complications in certain locations and unpleasant symptoms due to their growth and pressure accumulation with respect to surrounding tissues.[2] In such cases treatment often involves surgery, or radiation if the location is surgically inaccessible.

On the other side, malignant tumors also known as cancer are progressive diseases requiring prompt and adequate therapy.[1] Cancers show destructive invasive growth behavior resulting in blood loss, pressure and destruction of adjacent tissue, constriction of flow in vital organs and finally pathological metabolic changes in the body. Therapy may include surgery, radiotherapy, chemotherapy and/or biological therapy.[3] Most current guidelines for treatment of cancers include multimodal therapy along with management of side effects, and auxiliary treatment.

### 1.1.1 Epidemiology of cancer

Burden of cancer incidence conjointly grows with aging and growth of population.[4] The latest statistical report by the Czech National Cancer Registry (NOR) enumerates 87 361 new cases and 27 699 deaths from malignant neoplasms in 2018 in Czech Republic.[5] As reported by International Agency for Research on Cancer, globally, an estimated 18.1 million new cancer cases and

almost 9.9 million cancer deaths occurred in 2020. For the sake of using the more up-to-date information, following data will be analyzed in detail from a more global perspective. The number of new cancer cases and cancer deaths were extracted from the GLOBOCAN database of all cancers combined (thus, ICD-10 codes C00-C97), except nonmelanoma skin cancer (excluding basal cell carcinoma).[4]

Statistics of cancer are globally diverse.[4] Most diagnosed cancer cases leading to death are determined upon several main factors: sex, age-group, world region and its development indicated by 4-tier Human Development Index (HDI), a composite statistic of life expectancy, education and *per capita* income indicators. In men, prostate followed by lung, colorectal and liver cancer are most frequently diagnosed cancers, while lung cancer followed by prostate and liver cancer appear to be the most fatal. On the contrary, morbidity in women is given by breast and cervical cancers. Breast, cervical and lung cancer are considered top ranked in mortality in women. Incidence rates increased with increasing HDI (representing transitioned countries), and mortality is two-fold higher in the countries with higher HDI.

## 1.1.2 Risk Factors, early detection and prevention

As causes of cancer are not completely understood, to prevent it, we must mainly rely on risk factors that increase the chance of developing cancer.[6] According to American Cancer Society, more than 40% newly diagnosed cancers in US are potentially avoidable. Well-pronounced risk factors are smoking, obesity, poor nutrition, physical inactivity, alcohol consumption, psychosocial stress and lack of sleep, excess exposure to sunlight, and continual exposure to carcinogens in polluted air, water, or soil.[6,7] Other risk factors cannot be influenced like age, sex, and genetic susceptibility. Nevertheless, no matter what kind of risk factors or causes augmented the onset of cancer, early therapeutic intervention is key to a successful recovery.

To decrease the population burden of cancer, it is crucial to implement prevention and early detection strategies. Existing approaches are to be optimized, and some yet to be developed and research-spurred. However, just like the classification of cancers is complex, so is their mechanism-based risk assessment and intervention. The risks are not uniform across the population, but vary

according to age, genetic susceptibility, preneoplastic conditions and many unknown, untraceable factors.[8] Certain strategies are applied to general population, *e.g.*, smoking bans, HPV vaccination, colorectal, breast, lung and cervical cancer screening programs. Most other strategies rely on detecting and focusing on individuals at elevated or high risk of developing cancer, including individuals with preneoplastic lesions and targetable mutations – low-dose lung CT in some smokers, mammography in childhood cancer survivors, risk-reducing oophorectomy in *BRCA1/2* mutation carriers etc.

# 1.2 Targeting Cancer

## 1.2.1 Cancer hallmarks

Each cancer type results from a unique combination of germline and somatic mutations.[9] Currently, eight hallmarks have been proposed as the main distinctive and complementary biological capabilities acquired during the multistep development of human tumors along with two enabling factors (illustrated in
Figure 1).[10]

Specifically, cancer hallmarks are known as sustaining proliferative signaling, evading growth suppressors, resisting cell death, enabling replicative mortality, inducing angiogenesis, activating invasion and metastasis, reprogramming of energy metabolism and avoiding immune destruction.[10] Enabling factors are principal to these hallmarks, including genome instability and tumor-promoting inflammation.

Conceptual progress in the last decade now spans over two more emerging hallmarks and two further enabling factors: unlocking phenotypic plasticity and senescent cells, along with nonmutational epigenetic reprogramming and polymorphic microbiomes, respectively.[10]
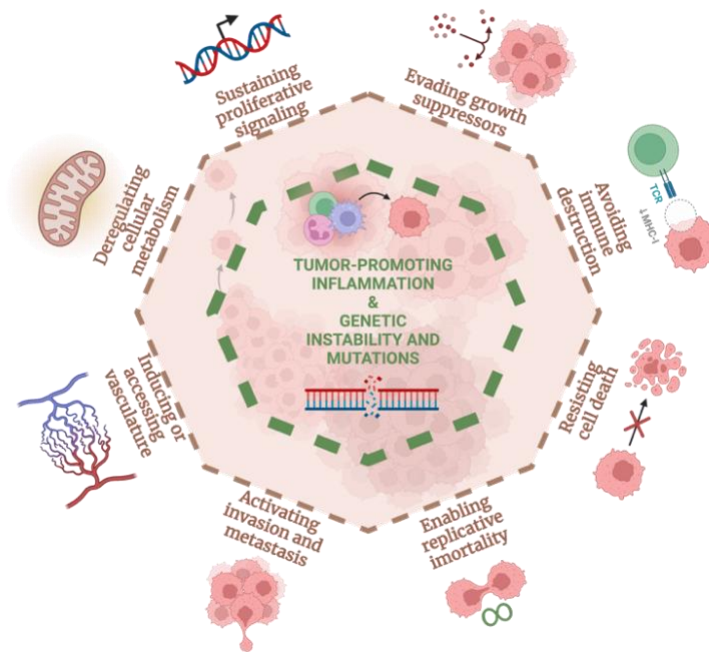
*Figure 1. Schematic representation of 8 hallmarks of cancer (in brown) and 2 enabling factors of cancer (in green). Created with Biorender. Adapted from ref.[10]*

It must be noted that tumors are not just insular masses of proliferating cancer cells, but complex tissues including tumor-associated normal cells, also contributing to carcinogenesis. Therefore, these hallmark traits are not just given by the cancer cell parenchyma but the tumor microenvironment (TME) as a whole.[11] Moreover, the TME is composed of an altered extracellular matrix and various non-cancer cells including cancer-associated fibroblasts, mesenchymal stem cells, endothelial cells, pericytes, vascular smooth muscle cells, adipocytes, tumor-infiltrating lymphocytes, and/or tumor-associated macrophages.[3] It has been proven that these cooperating cells may eventually depart from normalcy, coevolving with, and supporting growth of their malignant neighbors.[12]

### 1.2.2 Carcinogenesis

Carcinogenesis, also referred to as oncogenesis or mutagenesis, is the multistage and multistep process involving the modification and mutation of genes that regulate normal cellular function, including cell growth control processes.[13] Simply said, it is the formation process of cancer.

The aforementioned genetic instability has been considered to be a major enabling factor for the initiation of carcinogenesis and the development of a

number of degenerative diseases, predominantly related to aging.[14] Genetic information is a subject to constant attacks of various genotoxic insults, driven by both endogenous and exogenous agents.[15] Endogenous DNA damage sources include reactive oxygen species (ROS), a stalled replication fork and microbial metabolism products; on the other side, exogenous sources are, for instance, radiation, UV, and chemical carcinogens. Nevertheless, the cells possess many sophisticated mechanisms for response to such damage and DNA-induced checkpoints that temporarily halt cell cycle progression, providing a time window for the cell to repair the lesions.

Excessive DNA damage or deficient DNA repair would result in accumulating genomic disorders that ultimately contribute to cell death. When simultaneous events challenge the cell's repair capacity and the damage response is defective, that is when malignant transformations come in. The cell's fate is then determined by the balance between the amount of DNA damage and its repair capacity.[16] Alternately, a misrepair of single-strand (SSBs) and double-strand breaks (DSBs) of DNA may result in genome rearrangement. It is well recognized that the inherited mutations in genes involved in sensing or repair of DNA damages instigate the accumulation of genomic instability and are responsible for many types of familial cancer syndromes. In addition to the hereditary background, altered DNA damage responses have been observed in many types of precancerous lesions.[14]

## 1.2.3 The DNA damage response pathway

Following any amount of DNA damage, it is a duty of the DNA damage response (DDR) pathway to respond through cell cycle arrest and repair, premature senescence, or apoptosis.[17] The DDR pathway can be divided into three interconnected sections: sensors detecting DNA damage, a signal transducer that triggers signaling cascades and an effector that impedes DNA repair.[16] Which exact pathway for repair is going to be activated is orchestrated by the type of DNA damage (Figure 2.), although a different repair pathway may potentially compensate in the absence of the optimal repair pathway.[18]

The most common subtle lesions in DNA such as SSBs tend to be repaired by base excision repair (BER).[18] In the case of bulkier SSBs that deform the DNA

helical structure (bulky DNA adducts), nucleotide excision repair (NER) is initiated as it also includes the excision repair cross-complementing protein 1 (ERCC1) that then surrounds the lesion followed by replacement with normal DNA replication. DSBs must be alternatively repaired owing to the absence of a homologous template for new DNA synthesis. The first major pathway is homologous recombination (HR), which collects the information about lost homologous sequences from other parts of the genome and then repairs DSBs during the S/G2 cell-cycle phase. Alternatively, the error-prone nonhomologous end joining (NHEJ) pathway, which functions through all cell-cycle phases excluding the M-phase, directly rejoins the break ends together. Fifth major DDR pathway is mismatch repair (MMR), following damage derived from replication-associated errors. MMR corrects nucleotide misincorporation during DNA synthesis to prevent permanent DNA damage in dividing cells.
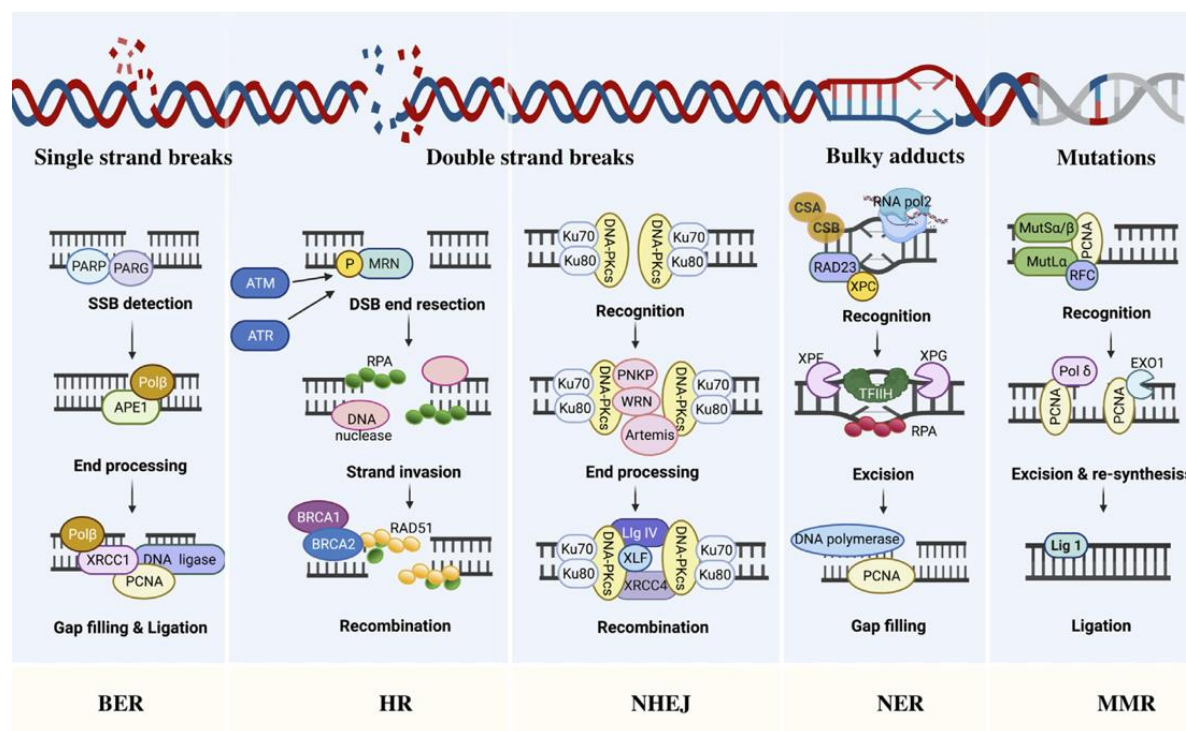


*Figure 2. Overview of stages in the five major pathways for the repair of DNA damage, by Wang et al. Taken from ref[16] licensed under CC by 4.0.; Base excision repair (BER); Poly(ADP-Ribose) polymerase (PARP); Poly(ADP-Ribose) glycohydrolase (PARG); DNA polymerase beta (Polβ); Apurinic/apyrimidinic endonuclease 1 (APE1); X-ray repair cross complementing protein 1/4 (XRCC1/4); Proliferating cell nuclear antigen (PCNA); Homologous recombination (HR); MRE11-RAD50-NBS1 complex (MRN); Ataxia telangiectasia mutated (ATM); Ataxia telangiectasia mutated and Rad3 related (ATR); Replication protein A (RPA); Breast cancer type 1/2 susceptibility protein (BRCA 1/2); Non-homologous end joining (NHEJ); DNA-dependent protein kinase catalytic subunit (DNAPKcs); Polynucleotide kinase-phosphatase (PNKP); Werner syndrome helicase (WRN); DNA ligase I/IV (Lig I/IV); XRCC-like factor (XLF); Nucleotide excision repair (NER); Cockayne*

The response thus also varies throughout the cell cycle reflecting the checkpoints at different stages as they include various key DDR factors regulating them (Figure 3).
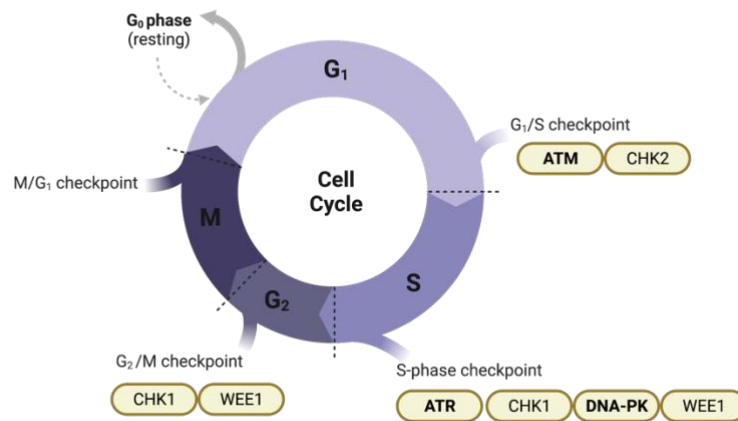


*Figure 3. DDR regulators as potential targets (yellow) throughout the cell-cycle, simplified. Targets shown in bold belong to PIKK family of kinases. Adapted from ref.[18]; CHK1(2), checkpoint kinase 1(2); ATM, ataxia-telangiectasia mutated; ATR, ataxia-telangiectasia and Rad3-related; DNA-PK, DNA-dependent protein kinase.*

## 1.2.4 Synthetic lethality

As mentioned above, defects in DDR are implicated in the initiation and progression of cancers. Thus, these defects are an attractive therapeutic opportunity to target cancers with minimum impact on normal cells as they have shown to be relevant to the effectiveness of standard treatment procedures, such as radio- and chemotherapy.[19] First approach to exploiting this property of cancer is to develop chemo- or radiosensitizers to help prevent and overcome resistance and, as a consequence, increase the effectiveness of standard genotoxic treatment. The second approach is to selectively eliminate a gene product that is synthetic lethal to a cancer-relevant mutation.

Calvin Bridges first described the paradigm of synthetic lethality in the context of *Drosophila Melanogaster,* where there were involved two genetic-loss-of-function events, either of which alone was compatible with viability but together

in the same cell resulted in lethality.[18] By today, this was put in context of anticancer treatments, and several synthetic lethal interactions were identified and characterized. Olaparib, a poly(ADP-ribose)polymerase (PARP) inhibitor for treating BRCA2-deficient breast and ovarian cancers, is the first drug based on this strategy to be approved.[20] Currently, as four PARP inhibitors are approved for use in anticancer treatment, encouraging results from exploiting the synthetic lethality concept lead to the development of further molecules inhibiting multiple different DDR pathways.[21] In parallel to the kinases featured in Figure 3, further DDR-modulating types of drugs in development and clinical trials for anticancer treatment are showing promising results as well: ataxia telangiectasia and Rad3-related (ATR) inhibitors, DNA-dependent protein kinase (DNA-PK) inhibitors, WEE1 inhibitors, and checkpoint kinase 1/2 (CHK1/2) inhibitors.

In this work, the concept is applied to the synthetic lethal interaction between ataxia-telangiectasia mutated (ATM) and ATR kinases (Figure 4).
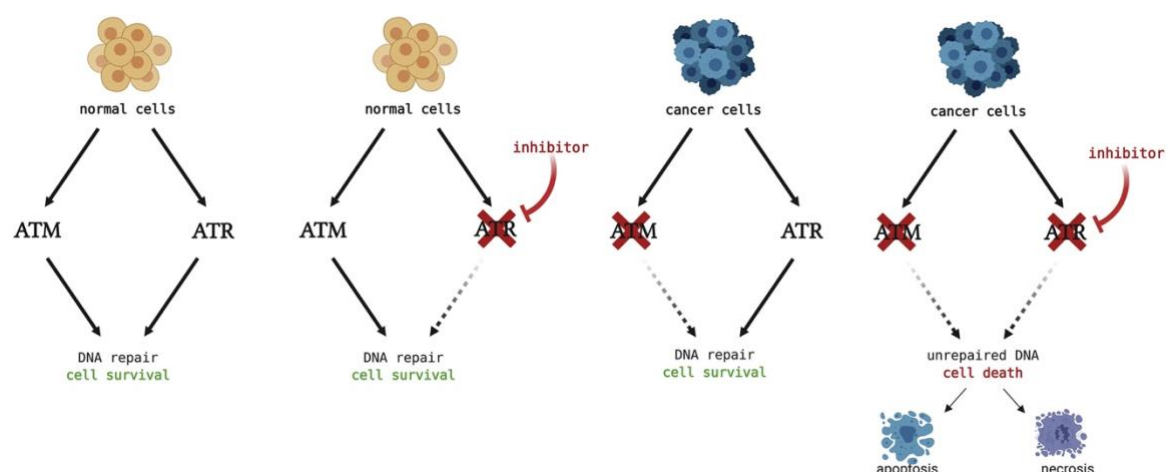


*Figure 4. Schematic representation of a synthetic lethal interaction between ATM and ATR kinases, by Gorecki et al. Taken from ref.[20]*

ATM is a tumor suppressor from the phosphatidylinositol 3-kinase-related kinases (PIKK) family, which commonly appears hypermethylated in cancers (and thus incapable of DNA repair). Prior activation, ATM remains in homodimer or higher-order multimers which dissociate into active monomers following rapid intramolecular autophosphorylation.[19] ATM's recruitment to chromatin is triggered by DSBs, more precisely by binding to the MRE11-RAD50-NBS1 (MRN) complex, or by reaction to oxidative stress and chromatin changes.[22] Subsequently, ATM phosphorylates directly or indirectly several downstream substrates including p53,

checkpoint kinases 1 and 2. It leads to G1/S (and partly G2/M and intra-S) cell cycle arrest (Figure 3). Of note, the transcription factor p53 is the most frequently mutated tumor suppressor gene in human cancer.[23] The ATM-p53 axis is therefore an important factor in aiming for G2 control through the synthetic lethal interaction with ATR.

## 1.3 ATR Kinase

ATR, another key apical PIKK participant involved in DDR, is on the other side activated by single-stranded DNA structures that arise *e.g.*, at resected DNA DSBs or stalled replication forks. This protein-kinase has been shown in several studies to be essential for development and viability of multicellular organisms as its activity is required during normal S-phase to ensure proper DNA replication and maintenance of genomic stability.[19] As most tumor cells have defective G1 cell-cycle checkpoint, they are reliant on the intra-S-phase and G2/M checkpoints to arrest the cell cycle, allow DNA damage repair, and consequently cell survival. Thus, ATR inhibition is a particularly attractive strategy for abrogating cancer survival.

Activation of ATR is a multistep process initiated upon DNA replication perturbation or DNA damage involving the presence of single-strand DNA (ssDNA).[20] The two pathways of ATR activation are presented in the Figure 5.
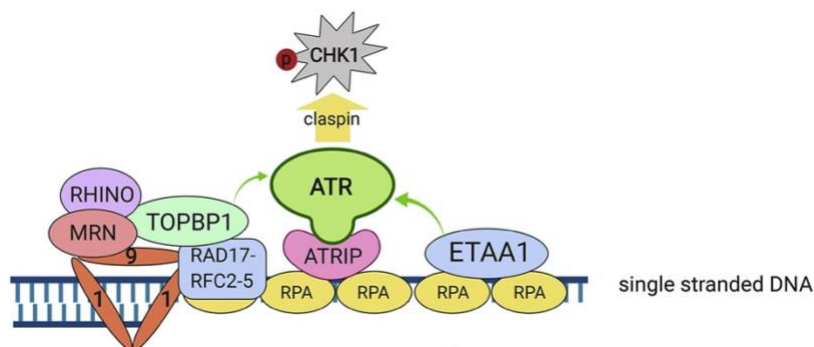


*Figure 5. Activation of the ATR-CHK1 pathway upon stalled replication fork, or during DNA end resection, by Gorecki et al. First activation step involves replication protein A (RPA) present on any ssDNA which directly calls ATR interacting protein (ATRIP) and ATR forming an inactive ATR-ATRIP complex. The complex is then activated through the ATR activating domain through the second step and undergoes a conformational change. The second pathway includes topoisomerase II binding protein 1 (TOPBP1) based on the presence of a single- or double-stranded DNA junction that serves as the loading point for the RAD9-RAD1-HUS1 (9-1-1) clamp complex, which is loaded onto DNA by RAD17-replication factor C subunits 2-5. The TOPBP1 protein is then recruited and activated through the MRN complex and RAD9-RAD1-HUS-interacting nuclear orphan*

ATR afterward phosphorylates a plethora of downstream mediators and effectors, mainly by its regulatory pathway via checkpoint kinase 1 (CHK1), as presented in Figure 6.[20] CHK1 is almost exclusively phosphorylated at Ser345 and, as such, serves as a potential biomarker for ATR inhibitor (ATRi) efficacy. Activated CHK1 leads through phosphorylation to proteasomal degradation of CDC25A, a phosphatase that removes inhibitory modifications from cyclin-dependent kinases (CDKs), thereby slowing down or arresting cell-cycle progression and restraining replication origin firing. Secondly, by targeting helicases such as SMARCAL1, ATR limits replication fork collapse. Thirdly, ATR regulates deoxyribonucleotide availability in mammalian cells by promoting the upregulation of ribonucleotide reductase subunit *RRM2* at the transcriptional and post-translational levels in response to DNA damage. ATR also facilitates the initiation of origin firing through minichromosome maintenance complex (MCM) or Fanconi anemia group I (FANCI). ATR inhibition hence results in a global depletion of RPA, DNA breakage, and ultimately a replication catastrophe.
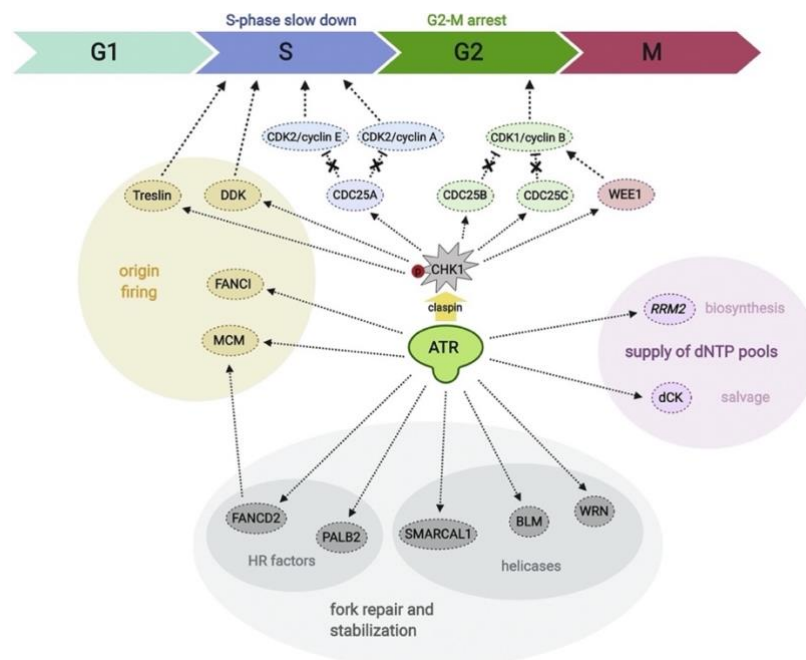


*Figure 6. Schematic representation of ATR's substrates and subsequent actions, by Gorecki et al. Taken from ref.[20]*

## 1.3.1  ATR inhibitors in (pre)clinical trials

The ATR kinase belongs to the PIKK serine/threonine kinase family along with ATM, DNA-PKcs, human suppressor of morphogenesis in genitalia-1 (hSMG-1), mammalian target of rapamycin (mTOR), and transformation/transcription associated protein (TRRAP).[24] Owing to their similar domain folding, clustering and many common structural features, it is common that certain DDR inhibitors intended for inhibition of other kinases also show activity towards ATR, and vice versa; thus, the development of a highly selective inhibitor can be problematic.[22] Furthermore, ATR was initially named FRAP-related protein 1 (FRP1) because of its similarity to the mTOR (originally FRAP).

The first molecules described to inhibit ATR were caffeine and schisandrin B; however, they did not suffice for clinical usage, as they either did not exhibit enough selectivity in relation to ATR compared to the rest of DDR PIKK family, or were not potent enough, respectively.[25] Afterwards, several other agents have shown inhibitory activity towards ATR, including compounds developed as inhibitors of other kinases in DDR *e.g.*, a CDK2 inhibitor NU6027 and a NVP-BEZ235 which was developed as PI3K and mTOR inhibitor (structures not shown).

Four ATRis have reached clinical trials: berzosertib, ceralasertib, elimusertib and gartisertib (Figure 7), with the -sertib suffix standing for serine threonine kinase inhibitors.[26] Regarding the results from their preliminary *in vitro* and *in vivo* studies, the effectivity of the compounds was, among others, evaluated in correlation with different synthetic lethal combinations and several possible susceptible mutations.

A double blockade on a single DDR pathway, for instance, has shown to be a strategy providing a synergistic effect substantially reducing tumor growth, and even being antimetastatic, as shown in experiments with berzosertib partnered with a CHK1 inhibitor or WEE1 inhibitor, respectively.[20] Many experiments were also conducted aiming at proving the chemosensitizing properties of ATRis to other DNA damaging agents. Firstly, platinum-based chemotherapeutics cause intra- and inter-strand crosslinks leading to cytotoxicity causing immediate DDR, thus also including activation of the ATR kinase. A similar concept can then be applied to gemcitabine, an antimetabolite nucleoside analogue stalling replication after integration into the growing DNA strand, or topoisomerase I and II inhibitors

(topotecan, irinotecan, indotecan, and etoposide) that cause SSBs and DSBs by inhibiting unknotting of DNA supercoils. ATR was also proven to play an important role in resistance to PARP inhibitors in BRCA-deficient cancer cells; thus, ATR inhibition can be exploited either as an alternative treatment in the resistant HR-deficient tumors or, as a synergic agent to the PARPi.[27] Preclinical studies also showed that exploiting DNA damage caused by radiotherapy is a useful tool in radiation-resistant hypoxic cancer cells, while also sparing healthy cells where no radiosensitization by ATRis occurred.[28]

Backtracking to the DDR pathways, ATM and p53 are not the only synthetically lethal DDR partners to ATR exploitable in cancer's high replication stress (RS) environment. VE-821, berzosertib's developmental precursor, was evaluated as monotherapy in cancer model bearing HR deficiencies related to ATM, *BRCA2*, X-ray repair cross-complemented protein 3 (XRCC3), or BER deficiencies.[20] Another study showed that cells with alternative lengthening of telomeres exhibit greater sensitivity to VE-821 than cells with active telomerase, suggesting that ATR inhibition can cause fragility of telomeres. Rational use of ATRis has moreover been backed up by synthetic lethal inactivating mutations in *XRCC1*, *BRCA1*, *BRCA2*, and *ARID1A* (AT-rich interactive domain-containing protein 1a), as well as proto-oncogenes that induce RS (*e.g.*, *MYC*, *KRAS*, or Cyclin E).

The four candidates are currently under clinical evaluation in patients with advanced solid tumors (including metastases), with ceralasertib and elimusertib also having indications in leukemias and lymphomas.[29] Berzosertib is administered intravenously due to poor peroral bioavailability, whereas the rest three have good peroral availability, hence can be dosed orally.[30]
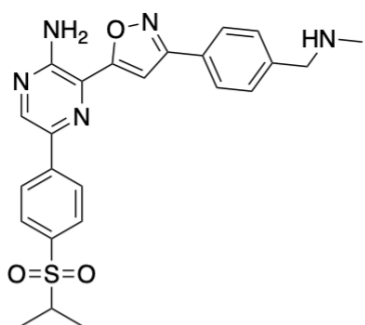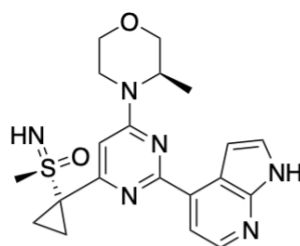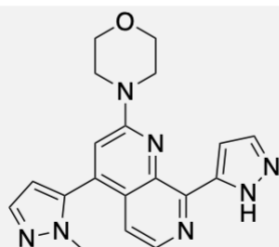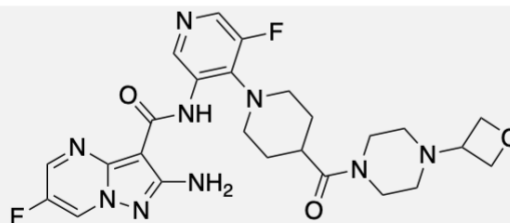
*Figure 7. Overview of ATR inhibitors currently in clinical trials (I/II); enzymatic inhibitory constants towards ATR (ATR Ki); cellular median inhibitory concentration towards ATR (cell IC$_{50}$). Data from ref.[31–34]*

With the first-in-class, berzosertib, several sets of results have been gathered from phase I trials. Firstly, a study where patients with small-cell lung cancer (SCLC) were administered a combination of topotecan and berzosertib, showed particular activity in platinum-refractory SCLC, which tends not to respond to topotecan alone.[35] In another trial, where berzosertib was assessed both as monotherapy and as a chemosensitizer to carboplatin in several different types of solid tumors, also showed that the ATRi is well-tolerated in both regimes and showed preliminary antitumor responses.[36] Similar results were confirmed in ongoing trial involving two different combinations: berzosertib with gemcitabine, and berzosertib with gemcitabine and cisplatin.[37] Other agents' combinations with berzosertib are being currently assessed in clinical trials *e.g.*, with cisplatin, radiation, paclitaxel, docetaxel, and veliparib.[20]

Ceralasertib has been predominantly tested both as monotherapy and in combination with PARPis, or gemcitabine or monoclonal antibodies (durvalumab), amongst other agents.[38,39] Results from phase I have also shown partial and complete responses in patients.

Elimusertib's results from preclinical studies have revealed strong antiproliferative activity, with good synergism when combined with olaparib, darolutamide (a nonsteroidal androgen receptor antagonist), pembrolizumab and BAY-2304058 (FGFR2-targeted thorium-227 conjugate). Preliminary data from phase I shows a good response in ATM-deficient tumors.

Gartisertib is the newest in the clinical setting, and its preclinical data is not extensively reported.

# 2  AIM OF THE WORK

This work aimed to synthesize novel compounds exerting anticancer activity in monotherapy and combinatorial regime. To achieve this goal, the plan was to design new compounds with structural frameworks based on known ATR inhibitors released into clinical trials.

The synthetic route includes Suzuki coupling, hydrolysis, and finally, the formation of amides containing 7-azaindole and 2,7-diazaindole core structures substituted with various amines on one side and methane- or isopropanesulfonylphenyl moiety on the other. Furthermore, the aim was to assess if the new core structures are feasible anticancer agents and to establish structure-activity relationships through a comparison of assessed anticancer activity and varying structural patterns.

# 3 RESULTS AND DISCUSSION

## 3.1 Design

To target ATR and thus generate new potential anticancer agents, the clinical candidate berzosertib and its main predecessor VE-821 along with all the structural frameworks associated with ATR-selective profile were chosen as template scaffolds applying structure-based drug design approach (Figure 8). Vertex Pharmaceuticals' PI3K homology model of the active ATR site developed from PDB entry 1E7V was applied for the design.[31]
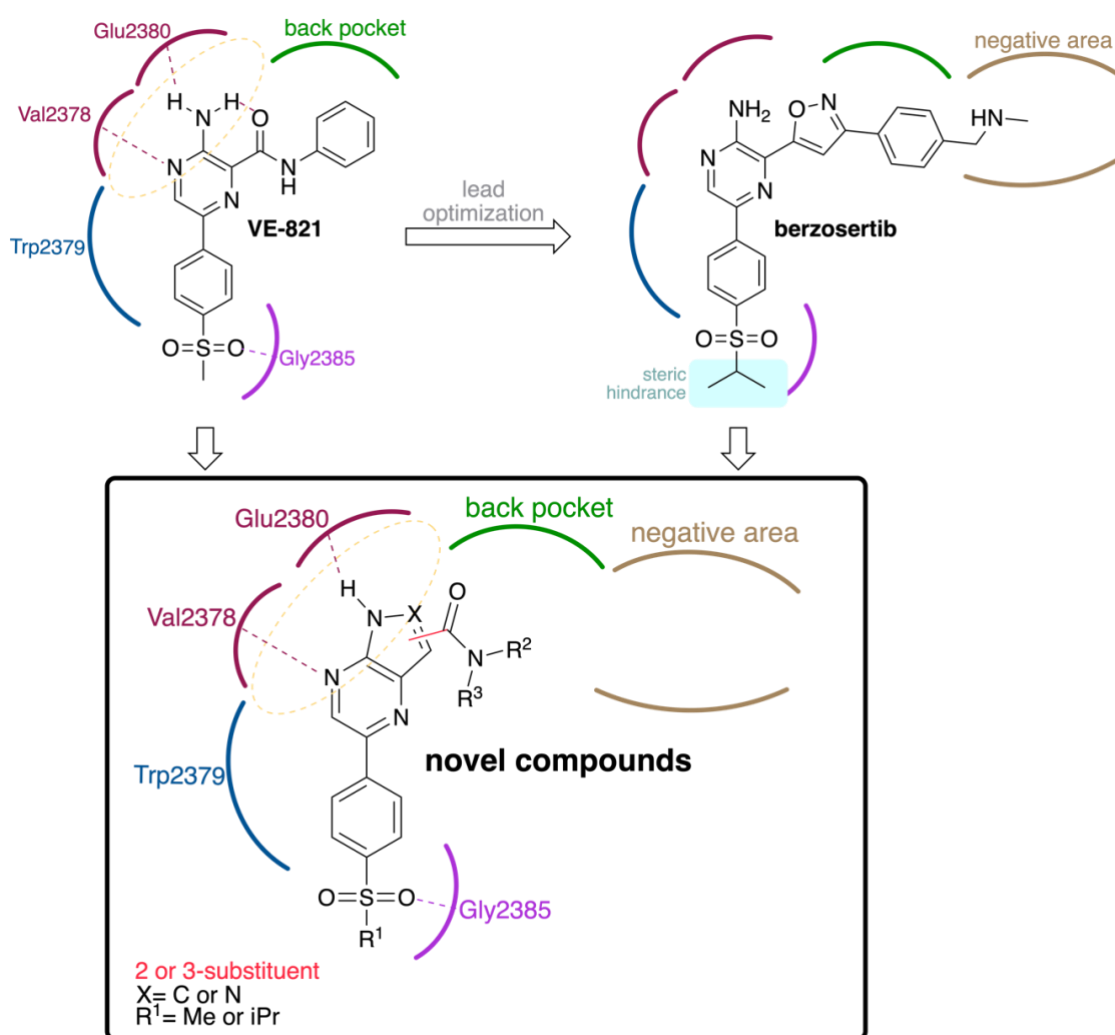


*Figure 8. Schematic representation of the crucial motifs responsible for ATR binding of VE-821 and berzosertib (upper part of figure); The binding presumptions for the 15 molecules prepared within this work (lower part of figure).*

The motifs crucial for ATR binding according to previous studies and our adaptation to the novel compounds (shown in Figure 8) are the following.

Pyrazine nitrogen in position 1- or morpholine oxygen (*e.g.*, in ceralasertib and elimusertib shown in Figure 7) are crucial hydrogen bond acceptors to interact with Val2378 in the hinge region.[31,40] The exocyclic amine at the position 2- on the pyrazine ring provides for both H-bond interactions with the carbonyl of Glu2380 and intramolecular H-bond with carbonyl or oxazole oxygen (in VE-821 and berzosertib, respectively) to ensure bioactive conformation. The heterocyclic pyrazine and a nitrogen of morpholine ring are essential for π-π and cation-π stackings, respectively, with the indole ring of Trp2379 in the ATP binding site pocket. In this work we molded all these motifs into two core structures: 7-azaindole and 2,7-diazaindole, presuming the ring closure approach to amino group from pyrazine core into bicyclic systems will ensure the H-bond and aromatic interactions, plus preserve the bioactive conformation.

Concerning the phenyl ring attached to the 2-aminopyrazine core, *para*-position was favored for the selectivity and highest affinity to ATR given the data from previous studies.[40] An aromatic ring in position 5- of pyrazine also provides π-π interactions with Trp2379. Another motif highlighted for its property of increasing the potency and selectivity against ATR is the alkanesulfonyl group with a bulkier alkyl chain, optimally an isopropyl moiety. Both the *para*- positioned and alkanesulfonyl moieties combined presume a hydrogen bond formation with the backbone N-H of Gly2385 which is specific to ATR, as ATM and DNA-PKc kinases contain a proline and threonine residues in this part of the peptide sequence, respectively. In our compounds, this part of molecule is presented as the 4-alkanesulfonylphenyl substituent on the position 5- of the 7-azaindole or 2,7-diazaindole core. Another key characteristic for an optimal fit in the cavity of the active site is the "L-shape" of the molecule. This can be explained with the ATR homology model, which suggests that the dihedral angle in the co-complex is ~65° for an optimal H-bond with Gly2385.

Regarding the back pocket under the P-loop (region rich in lipophilic residues), the aniline ring in VE-821 has shown to be an adequate binding prop. The main contributing counterpart is the aromatic ring with the anilide carbonyl functioning as a linker, proven *e.g.*, by later modification to the sole aromatic ring in berzosertib. In berzosertib a basic center in form of a secondary amine was further added, placing the molecule to an area of high negative charge delineated by residues Gly2385, Asn2480 and Asp2494. In our compounds, the amide group

was kept as an ideal planar tether that still could potentially provide additional H-bond interactions. The attached moieties were chosen to be aromatic and/or contain a basic center.
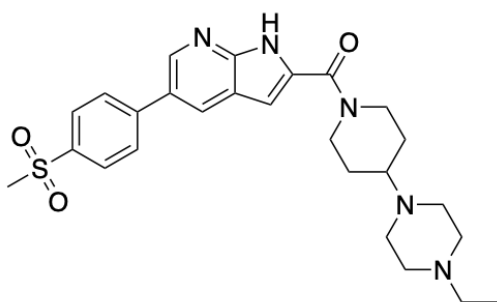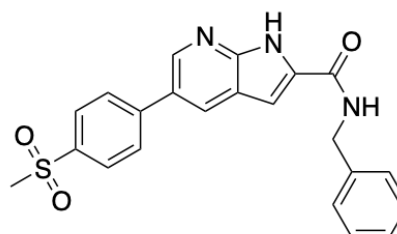
**C**

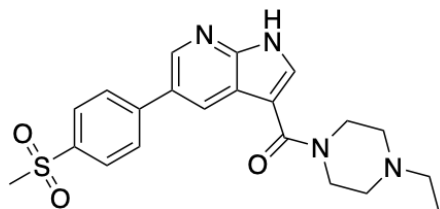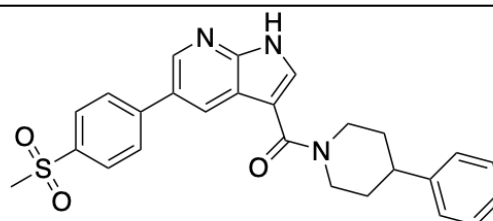**22**

**D**

**23**

**24**

**25**

**26**

**27**

**28**
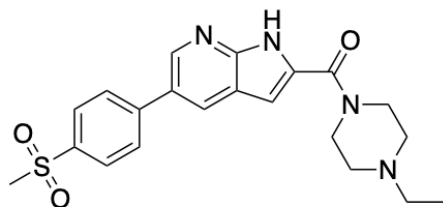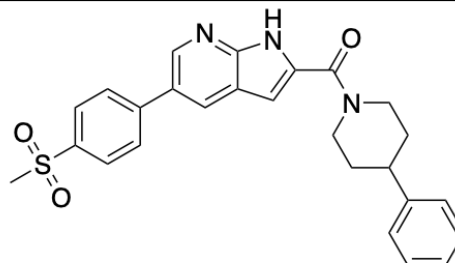
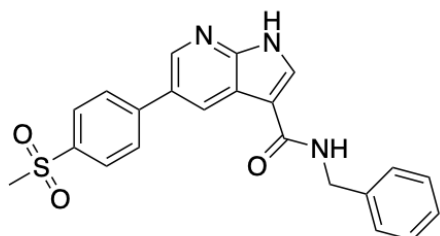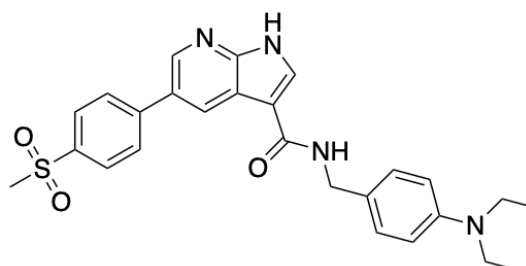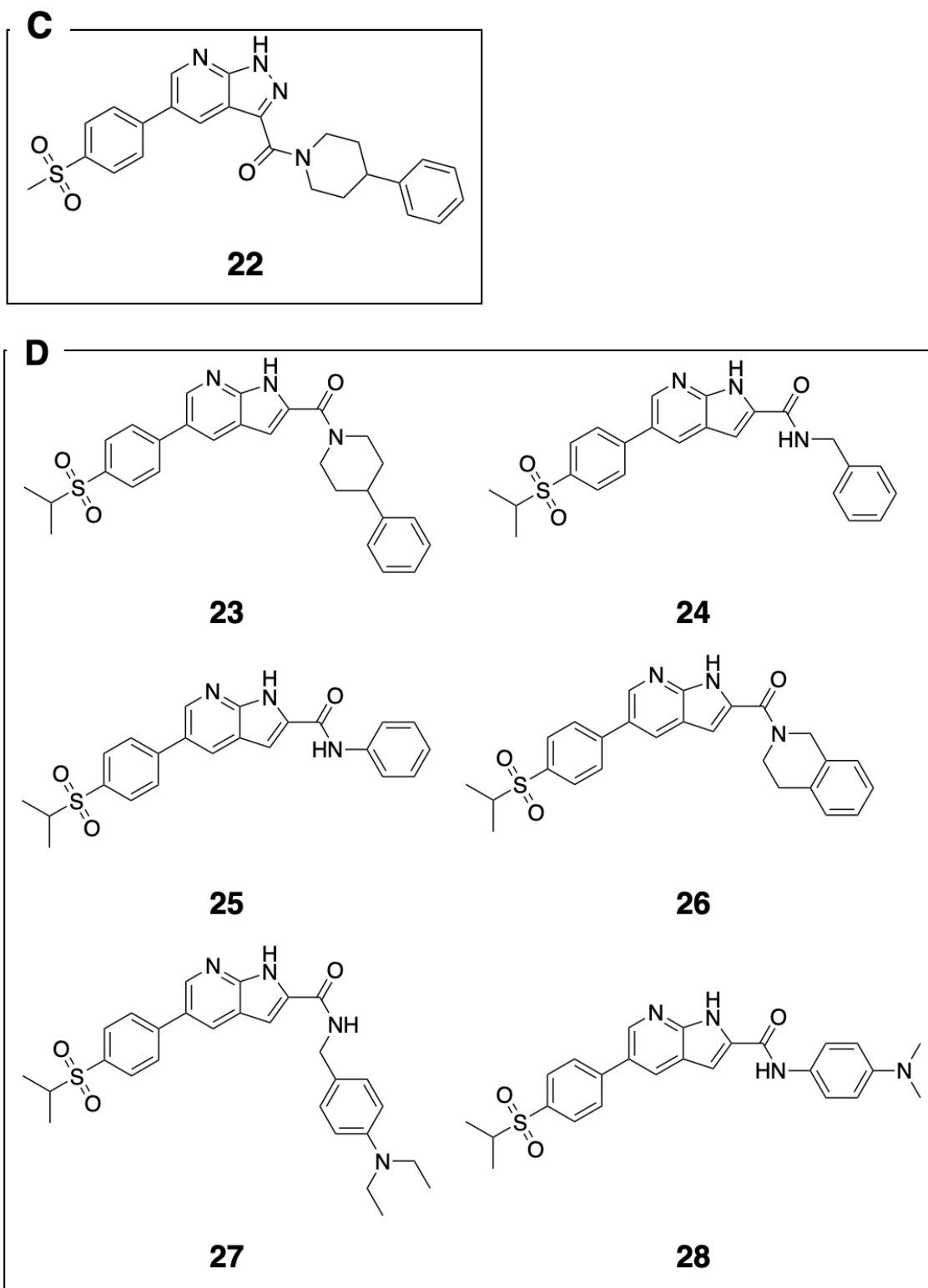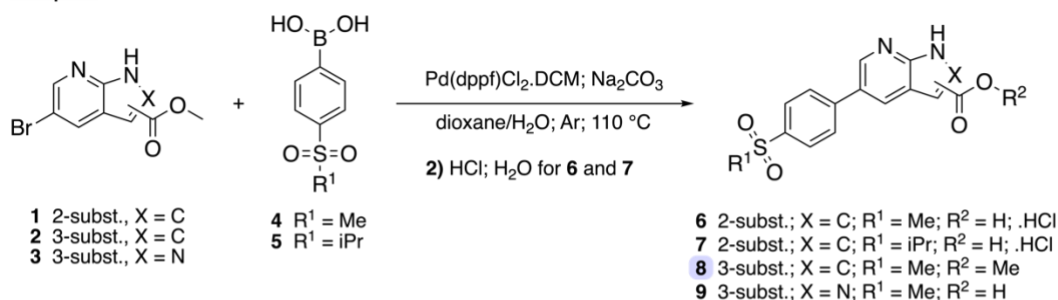*Figure 9. Overview of compounds synthesized in this work; **A** 2-substituted methanesulfonylphenyl 7-azaindoles; **B** 3-substituted methanesulfonylphenyl 7-azaindoles; **C** 3-substitued methanesulfonylphenyl 2,7-diazaindole; **D** 2-substitued isopropanesulfonylphenyl 7-azaindoles.*
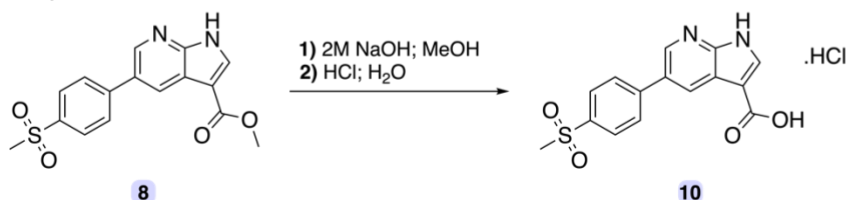
## 3.2 Chemistry

The novel ATRis presented in this work (Figure 9) were synthesized by a two-step procedure. In case of compounds **18**-**21** a three-step procedure was applied (Figure 10).
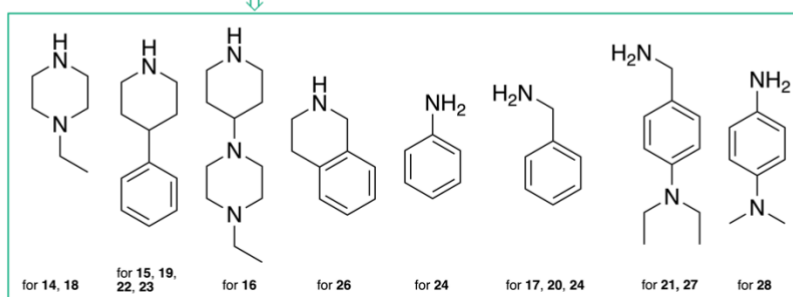


Step **A**

1 2-subst., X = C
2 3-subst., X = C
3 3-subst., X = N

4 R$^1$ = Me
5 R$^1$ = iPr

Pd(dppf)Cl$_2$.DCM; Na$_2$CO$_3$
dioxane/H$_2$O; Ar; 110 °C
2) HCl; H$_2$O for 6 and 7

6 2-subst.; X = C; R$^1$ = Me; R$^2$ = H; .HCl
7 2-subst.; X = C; R$^1$ = iPr; R$^2$ = H; .HCl
8 3-subst.; X = C; R$^1$ = Me; R$^2$ = Me
9 3-subst.; X = N; R$^1$ = Me; R$^2$ = H

Step **B**

1) 2M NaOH; MeOH
2) HCl; H$_2$O

8          10    .HCl

Step **C**

6 2-subst.; X = C; R$^1$ = Me; .HCl
7 2-subst.; X = C; R$^1$ = iPr; .HCl
9 3-subst.; X = N; R$^1$ = Me
10 3-subst.; X = C; R$^1$ = Me; .HCl

selected primary or secondary amine

EDC.HCl; HOBt.H$_2$O; DIPEA

14-17 2-subst.; X = C; R$^1$ = Me
18-21 2-subst.; X = C; R$^1$ = iPr
22 3-subst.; X = N; R$^1$ = Me
23-28 3-subst.; X = C; R$^1$ = Me

for 14, 18          for 15, 19, 22, 23          for 16          for 26          for 24          for 17, 20, 24          for 21, 27          for 28
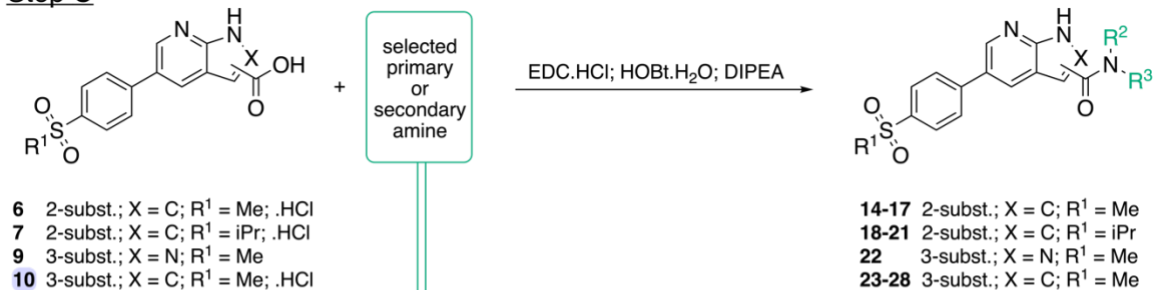
*Figure 10. Overview of the three steps representing the synthetic route to final compounds 14-28. More details about compounds and synthetic procedures can be found in the experimental section.*

In the step **A,** Suzuki-Miyaura reaction was used (Figure 11) involving a commercially available 5-bromo-substituted 7-azaindole, or 2,7-diazaindole with

29

methoxycarbonyl substituent in position 2-, or 3-, and organoborane compounds to form the alkanesulfonyl-core part of molecules. Sodium carbonate was used as a base and [1,1'-bis(diphenylphosphino)ferrocene]dichloropalladium(II) complex with dichloromethane as a palladium catalyst. Except for the reaction leading to compound **6** with 56% yield, the reaction proceeded well, with high yields (86% to 96%). Due to the Suzuki conditions, obtained esters **6**, **7** and **9** also hydrolyzed to carboxylic acids and were used as starting compounds in step **C**.
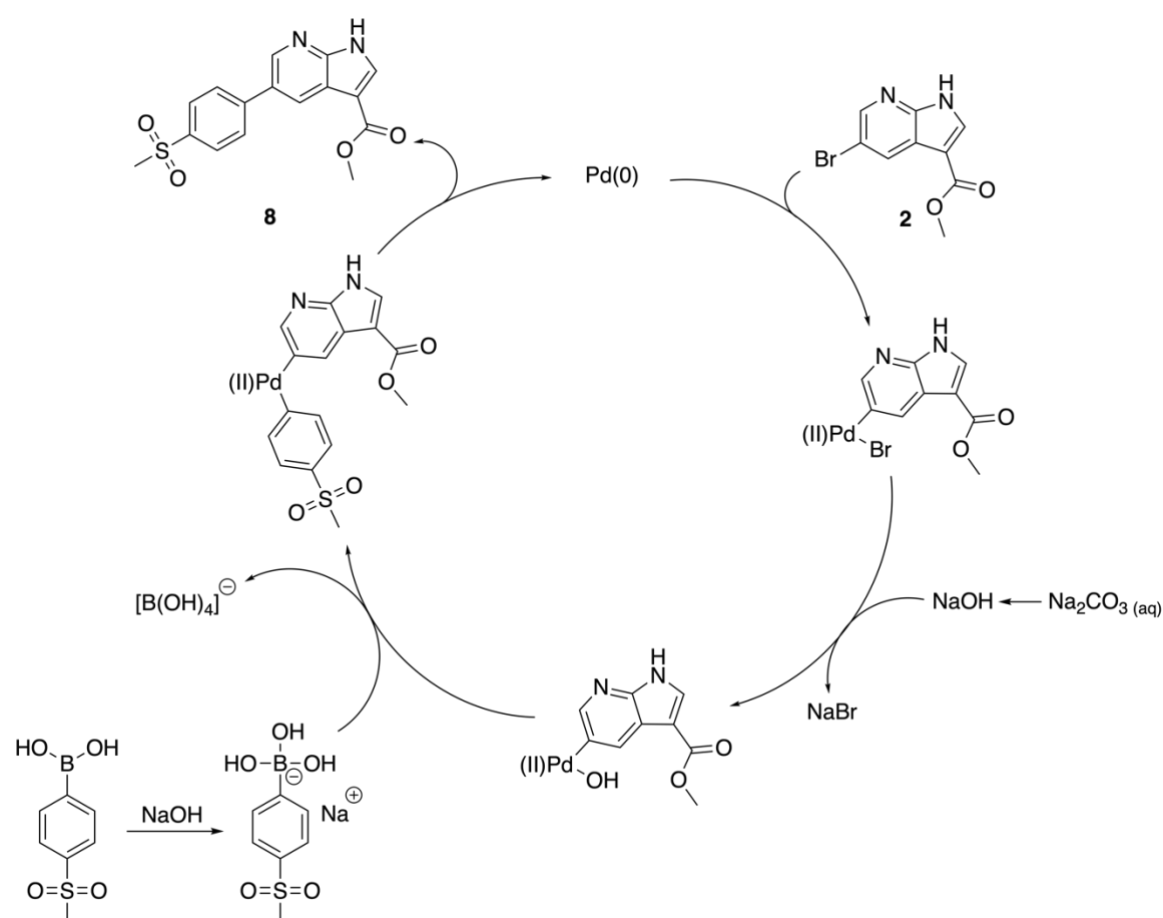


*Figure 11. Anticipated mechanism of the Suzuki-Miyaura reaction (the catalytic cycle) displayed on the example of the starting material 2, 4-(Methanesulfonyl)phenylboronic acid, and the corresponding product 8.[41]*

The 3-substituted methanesulfonylphenyl 7-azaindole **8,** on the other hand, remained stable in form of methylester and thus required a subsequent hydrolysis (step **B,** Error! Reference source not found.) before proceeding to acylation step **C**. The step **B** included hydrolysis to carboxylic acid **10** by NaOH in methanol at 110°C under reflux.

To form final compounds containing amide bond, carboxylic acids **6**-**10** were subjected to react with selected primary or secondary amines. 1-Ethyl-3-(3-

dimethylaminopropyl)carbodiimide (EDC) and hydroxybenzotriazole (HOBt) were used as a catalyst and activator of the starting acids (Figure 12).
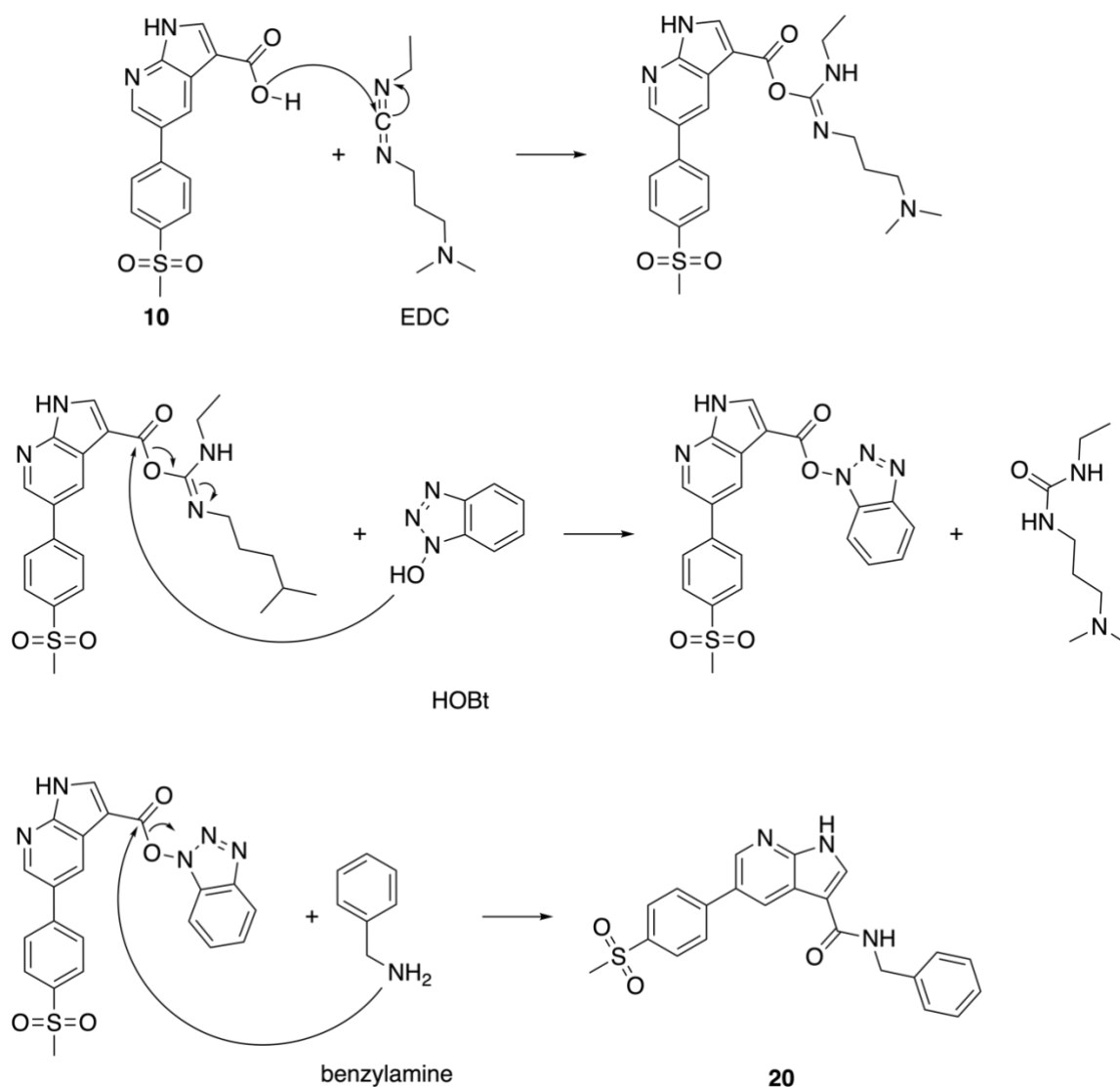


*Figure 12. Formation of amide (20) in the presence of EDC/HOBt from starting carboxylic acid (10), simplified. EDC reacts with the carboxylic acid group to form an active O-acylisourea intermediate that is displaced by HOBt forming an active ester and a soluble urea byproduct from EDC. An activated ester is then susceptible to the nucleophilic attack of amino groups in the reaction mixture, yielding the desired amide, herein compound 20. The reaction was executed in solvent tetrahydrofuran (THF) under basic conditions mediated by N,N-diisopropylethylamine (DIPEA). [42]*

The yields in step **C** varied from 20% up to 73%. Lower yields in some cases can be explained by the various work-ups needed as some of the final compounds were insoluble in most solvents. The extremely low solubility of some compounds was apparent in the first attempts of column chromatography, where the product retained in the column and was very unwillingly eluted in organic solvents. Based

on this observation, we modified work-ups in the subsequent reactions. In the cases where the compounds were expected to be more soluble (less aromatic rings, more basic centers, or more hydrophilic moieties), the workup proceeded with purification through column chromatography. In contrast, with the less soluble products, precipitation in MeOH and follow-up filtration was selected.

## 3.3 Biology

### 3.3.1 Cytotoxicity screening

The screening was conducted in collaboration with the Faculty of Medicine in Hradec Králové under the supervision of prof. Řezáčová and dr. Darina Muthna. To provide full insight into the activity/potential anticancer efficacy of these compounds, biological activities are disclosed herein, although, they were not performed by me.

All of the novel compounds **14-28** were submitted to *in vitro* screening at 10 µM concentration for a cytotoxic effect against nine selected cancer cell lines (two represent leukemic malignancies, and the rest are solid tumors) and one non-cancer cell line. The cell lines are listed with their mutation and p53 status in Table 1.

*Table 1. Short descriptions and specificities of cell lines (cancer in orange and non-cancer in blue) used to screen cytotoxicity of final compounds synthesized in this work. Data from database downloadable at http://p53.fr/*

| cell line | description | mutations and p53 status |
|-----------|-------------|--------------------------|
| Jurkat | acute T-cell leukemia | p53-mutation |
| MOLT-4 | acute lymphoblastic leukemia | controversial status |
| A549 | lung adenocarcinoma (NSCLC) | p53-wild type |
| HT-29 | colorectal adenocarcinoma | p53-mutation |
| PANC-1 | pancreas ductal adenocarcinoma | p53-mutation; **CDKN2 deletion** |
| A2780 | ovarian endometrioid adenocarcinoma | p53-wild type; **ATM mutation** |
| HeLa | cervix adenocarcinoma | p53-wild type (low expression) |
| MCF-7 | breast adenocarcinoma | p53-wild type; **CDKN2 deletion** |
| SAOS-2 | osteosarcoma | p53-mutation |
| MRC-5 | lung fibroblast – non cancer cells | - |

The non-cancer cell line MRC-5 was selected as a representative of healthy cells, where the cytotoxic or chemosensitizing effect is not desirable. The mutations in *TP53* (Jurkat, PANC-1, HT-29, SAOS-2), *CKDN2* (PANC-1, MCF-7) and *ATM* (A2780) are to be taken into account as these deficiencies should impact the efficacy of potential ATR inhibitors by several mechanisms such as loss of synergism with ATR, defect in G1/S control and HR deficiency, respectively.[16,43,44]

As mentioned in the introduction, ATRis are designated as chemosensitizing agents, especially for cancer therapy regimens that tend to develop chemoresistance over time.[45] For evaluation of compounds **14-28** (10 µM) in the combinatorial regimen, cisplatin (CDDP) was selected. CDDP is employed in treatments of a wide array of solid and leukemic malignancies where its main mechanism is the generation of intra- and inter-strand lesions by interacting with purine bases on DNA, resulting in DSBs and SSBs that rely on repair mechanisms orchestrated by ATR. In the assay, the concentration of CDDP was determined depending on its activity in specific cell lines.

Regarding the single-agent mode of treatment (Table 2A), compound **19** showed the highest overall cytotoxicity with average mean of remaining cell viability in all cancer cell lines of 49%. The cytotoxicity is apparently higher than in case of VE-821 in all cancer cell lines except for HT-29, whereas the proliferation in the healthy cell line was not reduced as well. The inactivity or very low activity towards MRC-5 is moreover a feature of all other assessed potential ATRis. The three most sensitive cancer cell lines (Jurkat, MCF-7 and SAOS-2) bear mutations either in *TP53* or *CDKN2*. The second top-ranked cytotoxic compound is **26,** whose overall cytotoxicity is also comparable to that of VE-821 (71% vs 66%); however, this is given mainly by the cytotoxicity towards the A2780 and Jurkat cancer cell lines. Both cell lines also bear at least one relevant mutation, either in *TP53* or in *ATM* genes. The third compound, regarding single-agent mode, with comparable cytotoxicity in several cancer cell lines compared to VE-821 is the **21**.

When it comes to the combinatorial regimen (results shown in Table 2B) the efficacy of novel compounds was considerably lower compared to VE-821. Only moderate cytotoxic effect in combination with CDDP was exerted by compounds **19** and **21**, followed by **26**, **27**, **14**. Nevertheless, several differences in sensitivity of cell lines as compared to the single-agent regimen can be observed. The healthy cell line was critically more suppressed, which can be attributed to CDDP's activity.

The SAOS-2 was significantly more sensitive to the combination of ATRi and CDDP along with the A549 cancer cell line, which previously showed almost no sensitivity to any of the ATRis alone. No correlation regarding the p53 status was observed.

*Table 2. **A:** Heat map for single-agent therapy (10 µM) against nine cancer cell lines and MRC-5, including positive controls VE-821 (10 µM) and cisplatin (CDDP; 2 µM for MOLT-4, Jurkat, A2780; 10 µM for MCF-7, MRC-5; and 15 µM for A549, SAOS-2, PANC-1, HT-29, HeLa). Values in each colored box show assessed viability of cell lines exposed to the ATRi (in bold at the top of column). Red color represents the most toxic compounds (reduction of proliferation to 1%), and the light blue represents no toxicity (>100% proliferation). **B**: Heat map for combinatorial regimen of each compound (10 µM) and CDDP (2 µM for MOLT-4, Jurkat, A2780; 10 µM for MCF-7, MRC-5; and 15 µM for A549, SAOS-2, PANC-1, HT-29, HeLa). Values in each colored box show assessed viability of cell lines exposed to the ATRi with CDDP. Red color represents the most toxic compounds (reduction of proliferation to 1%), and the blue represents no toxicity (100% proliferation).*

| A | 14 | 15 | 16 | 17 | 18 | 19 | 20 | 21 | 22 | 23 | 24 | 25 | 26 | 27 | 28 | VE-821 | CDDP |
|---|----|----|----|----|----|----|----|----|----|----|----|----|----|----|----|--------|------|
| Jurkat | 85 | 86 | 87 | 90 | 95 | 29 | 77 | 57 | 104 | 84 | 86 | 95 | 45 | 92 | 105 | 34 | 43 |
| MOLT-4 | 118 | 113 | 108 | 109 | 95 | 45 | 98 | 76 | 125 | 116 | 134 | 133 | 90 | 125 | 142 | 52 | 57 |
| A549 | 86 | 87 | 100 | 105 | 102 | 63 | 99 | 75 | 89 | 90 | 95 | 101 | 68 | 88 | 110 | 87 | 51 |
| HT-29 | 91 | 97 | 105 | 104 | 94 | 88 | 94 | 88 | 88 | 93 | 95 | 99 | 79 | 103 | 105 | 81 | 84 |
| PANC-1 | 90 | 104 | 110 | 105 | 97 | 41 | 88 | 107 | 102 | 109 | 107 | 109 | 101 | 103 | 105 | 87 | 71 |
| A2780 | 98 | 89 | 104 | 99 | 97 | 55 | 86 | 66 | 83 | 95 | 112 | 114 | 38 | 99 | 110 | 68 | 74 |
| HeLa | 84 | 94 | 83 | 96 | 95 | 51 | 91 | 66 | 82 | 82 | 85 | 95 | 76 | 76 | 99 | 75 | 63 |
| MCF-7 | 76 | 70 | 77 | 90 | 88 | 38 | 86 | 73 | 67 | 73 | 87 | 87 | 69 | 75 | 98 | 39 | 81 |
| SAOS-2 | 81 | 95 | 88 | 98 | 88 | 32 | 82 | 76 | 85 | 85 | 94 | 96 | 69 | 93 | 100 | 74 | 39 |
| MRC-5 | 114 | 102 | 127 | 124 | 121 | 100 | 118 | 105 | 100 | 102 | 119 | 117 | 89 | 98 | 133 | 116 | 30 |

| B | 14 | 15 | 16 | 17 | 18 | 19 | 20 | 21 | 22 | 23 | 24 | 25 | 26 | 27 | 28 | VE-821 |
|---|----|----|----|----|----|----|----|----|----|----|----|----|----|----|----|--------|
| Jurkat | 56 | 69 | 54 | 52 | 65 | 31 | 58 | 52 | 78 | 65 | 56 | 59 | 50 | 58 | 59 | 2 |
| MOLT-4 | 61 | 71 | 57 | 71 | 64 | 38 | 65 | 60 | 85 | 71 | 60 | 62 | 66 | 74 | 67 | 1 |
| A549 | 49 | 44 | 62 | 58 | 59 | 49 | 53 | 40 | 48 | 45 | 47 | 54 | 40 | 28 | 56 | 18 |
| HT-29 | 78 | 85 | 91 | 94 | 93 | 78 | 80 | 80 | 76 | 77 | 73 | 77 | 71 | 81 | 84 | 17 |
| PANC-1 | 70 | 79 | 78 | 82 | 84 | 37 | 71 | 65 | 77 | 81 | 74 | 76 | 74 | 76 | 79 | 34 |
| A2780 | 64 | 74 | 76 | 77 | 72 | 50 | 67 | 59 | 63 | 66 | 73 | 76 | 53 | 68 | 76 | 39 |
| HeLa | 57 | 70 | 72 | 79 | 70 | 52 | 60 | 69 | 98 | 60 | 59 | 62 | 57 | 40 | 64 | 3 |
| MCF-7 | 59 | 59 | 75 | 93 | 77 | 36 | 83 | 66 | 65 | 66 | 73 | 82 | 61 | 64 | 85 | 25 |
| SAOS-2 | 32 | 42 | 38 | 44 | 49 | 27 | 44 | 44 | 45 | 42 | 35 | 40 | 37 | 23 | 40 | 7 |
| MRC-5 | 26 | 30 | 31 | 36 | 36 | 50 | 38 | 33 | 29 | 33 | 31 | 38 | 30 | 28 | 34 | 28 |

Unfortunately, chemosensitizing properties throughout our screening were not observed, and the combinatorial regimen usually had only additive effects. By the extent of combinations, compounds **19** and **27** were the most prominent in certain cell lines with MCF-7 as the most susceptible.

Next, we established a structure-activity relationship (SAR). Starting with the core of ATRis, the most cytotoxic compounds belong to the 3-substituted 7-azaindoles (**18**-**21**, Figure 9), not distinguishing between primary or secondary amine tethered to the core structure. In all regimens, 1-phenylpiperidine compounds (**15**, **19**, **22**, **23**) displayed the highest cytotoxic effect, followed by the benzylamine-containing compounds **21** and **27** and further followed by compound **26** substituted with 1,2,3,4-tetrahydroisoquinoline which was interestingly superior to the 1-phenylpiperidine compound **23**. In the context of the presented compounds, the isopropanesulfonyl derivatives (**23**-**28**) showed slightly more cytotoxicity towards the healthy cell line, than their methanesulfonyl counterparts (**14**-**21**).

## 3.3.2 Efficacy against glioblastoma

This screening was conducted in collaboration with Biomedical Research Centre. To provide full insight of these compounds, biological activities were incorporated, although, they were not performed by me.

All compounds (**14**-**28**) are a part of a small library of 40 novel ATRis curated by supervisor dr. Górecki, out of which 7 compounds were selected for an additional screening on a secondary astrocytoma cell line (1321N1) and primary glioblastoma (GBM) cell line (Figure 13). Only compound **26** was elected into selection against brain tumor screening. Cell lines were assessed both in single-agent and combinatorial regimens with temozolomide (TMZ).

Glioblastoma multiforme is the most common malignant brain tumor in adults and is characterized by rapid progression, a high recurrence rate and poor prognosis.[46] TMZ (an alkylating agent) quickly became and remained a first-line medication upon its discovery; however, the development of resistance has also become the limiting factor in effective treatment. While the MGMT ($O^6$-methylguanine methyltransferase) repairs activity is an already well-known contributor to resistance, DDR pathways including G1 control defects have also come to light as molecular mechanisms granting resistance to TMZ in many populations. Treatment with ATR inhibitors and chemosensitization could thus potentially benefit these populations of patients.

Concerning efficacy of **26** towards to the 1321N1 cell line (Figure 13A), the results were in accordance with the previous screening where almost no chemosensitizing effect was observed. On the other side, the viability of the GBM cell line decreased almost to 50% (Figure 13B) and as such showed slightly higher but statistically insignificant cytotoxicity at 15 µM than TMZ alone at 1 mM. The chemosensitizing effect though, was not confirmed in this cell line either.
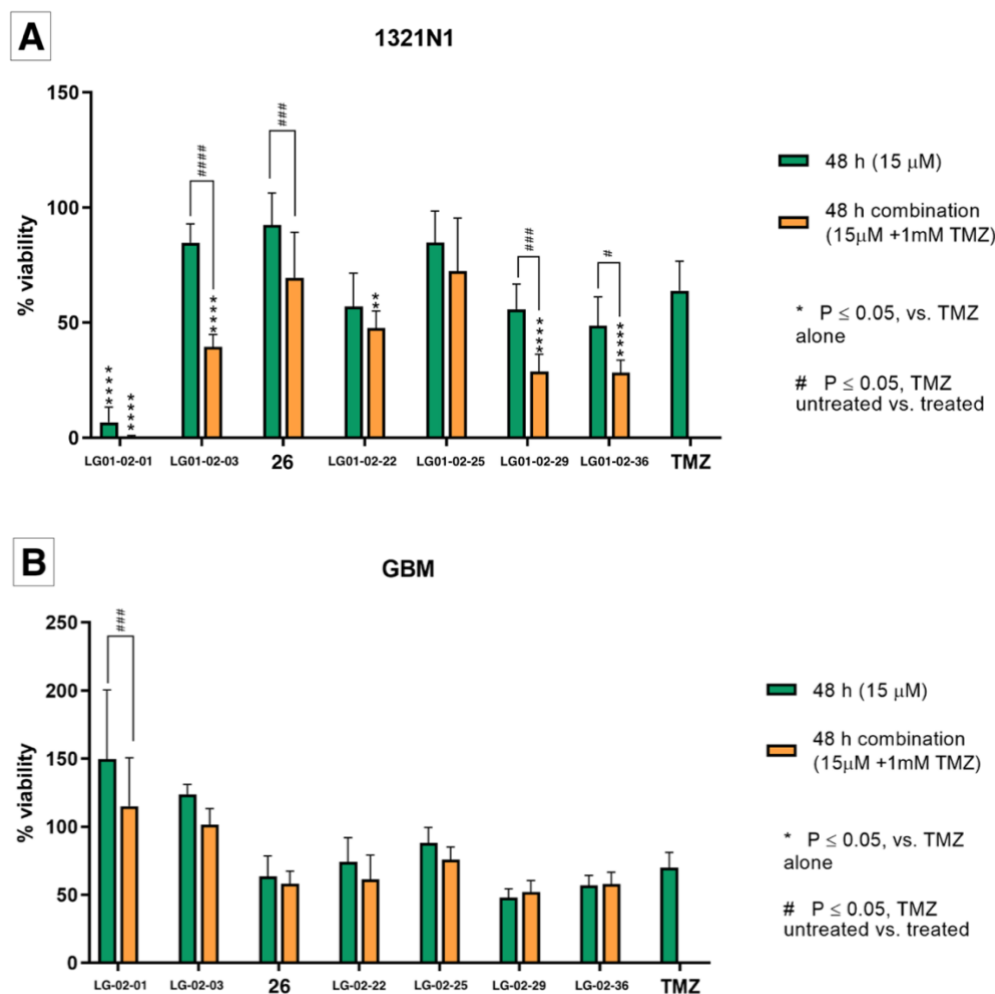


*Figure 13. Effect of compound **26** and six selected compounds (prepared by dr. Górecki (labeled LG-02-XX) from the same library of compounds) on secondary astrocytoma cell line 1321N1 (**A**) and primary glioblastoma cell line (**B**) in a single-agent therapy and in a combinatorial regimen with TMZ. Incubation time was 48h. Novel compounds were tested at 15 µM, TMZ at 1 mM concentration. The Dunnet´s and Sidak´s multiple comparisons tests were used to determine the significance of the difference between novel compounds or the combinations with TMZ vs TMZ alone (\*) and between novel compounds vs its combination with TMZ (#).*

# 4 CONCLUSION

One of the crucial enabling characteristics of cancer development is genome instability and mutations, often tightly connected to aberrant DNA damage response. Such insufficiency favors several kinases for targeting in a synthetic lethality manner. Among them, we highlighted ATR as our goal target for inhibition.

15 novel molecules with the 7-azaindole and 2,7-azaindole core were designed, synthesized, and subsequently submitted to *in vitro* cytotoxicity assays to quantify their activity.

The synthetic route leading to the final compounds, through Suzuki coupling and EDC/HOBt acylation, is efficacious and straightforwardly attainable. Although the latter step and its work-up methods were problematic, we were able to optimize reaction processing up to good yields > 60%.

Four miniseries of final compounds were prepared: **A:** four 2-substituted methanesulfonylphenyl 7-azaindoles; **B:** four 3-substituted methanesulfonylphenyl 7-azaindoles; **C:** one 3-substituted methanesulfonylphenyl 2,7-diazaindole; and **D:** six 2-substituted isopropanesulfonylphenyl 7-azaindoles.

*In vitro,* compounds **19**, **26**, and **21** showed comparable or higher cytotoxicity than VE-821 in monotherapy. In the combinatorial regimen with CDDP, the cytotoxicity was significantly lower than it is the case of VE-821 paired with cisplatin. Similarly in the glioblastoma cell line, compound **26** showed high cytotoxicity in monotherapy, whereas insignificant in combination with temozolomide.

The rationale for the new ATR inhibitors has thus shown to be effective in this type of treatment, albeit the chemosensitizing properties were not confirmed.

# 5 EXPERIMENTAL SECTION

## 5.1 General Methods

Chemicals were purchased from Sigma-Aldrich Co. LLC or Fluorochem Ltd. and were used without additional purification.

The analytical thin-layer chromatography was carried out using plates coated with silica gel 60 with a fluorescent indicator F254 (Merck, Prague Czech Republic). Thin-layer chromatography plates were visualized by exposure to ultraviolet light (254 nm).

The column chromatography was performed using silica gel 100 at atmospheric pressure (70 – 230 mesh ASTM, Fluka, Prague Czech Republic).

NMR spectra were recorded on a Varian S500 spectrometer and on a Bruker Avance Neo 500 (500 MHz for $^1$H and 126 MHz for $^{13}$C), and on a Jeol JNM-ECZ600R (600 MHz for $^1$H and 151 MHz for $^{13}$C). Chemical shifts are reported in δ ppm referenced to solvent residual peak standards for $^1$H and $^{13}$C NMR CD$_3$OD (CH$_3$OH-$d_4$; 3.35, 4.78 (H), 49.3 (C) ppm), or hexadeuteriodimethylsulfoxide (DMSO-$d_6$; 2.50 (D), 39.7 (C) ppm).

The final compounds were analyzed by LC-MS consisting of UHLPC Dionex Ultimate 3000 RS coupled with Q Exactive Plus orbitrap mass spectrometer (Thermo Fisher Scientific, Bremen, Germany) to obtain high resolution mass spectra. Gradient LC analysis confirmed > 95% purity.

## 5.2 Synthesis of Novel Compounds

### 5.2.1 General procedure A: Suzuki coupling reaction



**1** 2-subst., X = C
**2** 3-subst., X = C
**3** 3-subst., X = N

**4** $R^1$ = Me
**5** $R^1$ = iPr

**6** 2-subst.; X = C; $R^1$ = Me; $R^2$ = H; .HCl
**7** 2-subst.; X = C; $R^1$ = iPr; $R^2$ = H; .HCl
**8** 3-subst.; X = C; $R^1$ = Me; $R^2$ = Me
**9** 3-subst.; X = N; $R^1$ = Me; $R^2$ = H
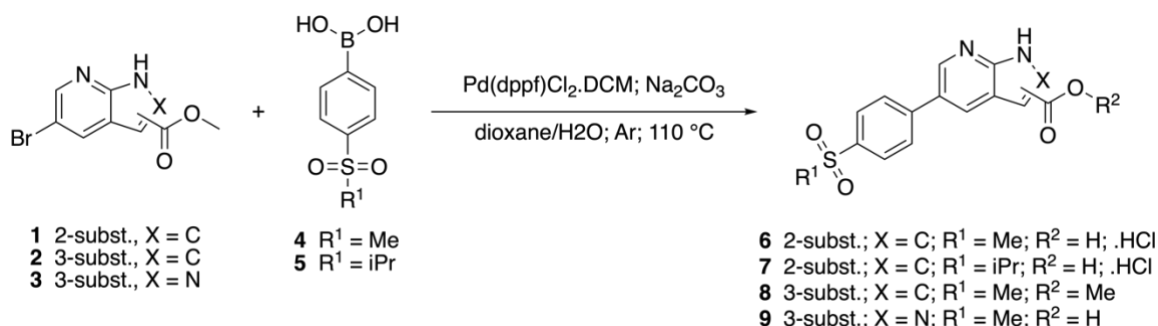
To a stirring solution of ester **1-3** (1.0 eq) in anhydrous 1,4-dioxane under Ar, boronic acid **4** or **5** (1.3 eq) was added under Ar. Then, 3M solution of sodium carbonate ($Na_2CO_3$; 10.0 eq) in Ar treated $H_2O$, and Pd(dppf)Cl$_2$.DCM (0.01 eq) were added subsequently, and the reaction mixture was heated to 110 °C for three days. After cooling, dioxane was removed by rotary evaporator, and the residue was diluted by $H_2O$ (100 mL). Aqueous phases of carboxylic acids **6**, **7**, and **9** were washed three times by ethyl acetate (EA; 3x 100 mL), and then three times washed by dichloromethane (DCM; 3x 100 mL). Resulting aqueous phase was carefully acidified by 10% hydrochloric acid (HCl) to pH ≈ 1. Precipitates were filtered and washed by additional $H_2O$ (3x 20 mL) and then by hexane (3x 20 mL) to get products **6** and **7** as hydrochloric salts and product **9** as a neutral compound.

Aqueous phase of ester compound **8** was three times washed by EA (3x 100 mL). The combined organic phases were dried over anhydrous sodium sulphate ($Na_2SO_4$), filtered, concentrated, and directly used in the subsequent hydrolysis reaction.

Starting materials:
**Methyl-5-bromo-1H-pyrrolo[2,3-b]pyridine-2-carboxylate (1)**
**Methyl-5-bromo-1H-pyrrolo[2,3-b]pyridine-3-carboxylate (2)**
**Methyl-5-bromo-1H-pyrazolo[3,4-b]pyridine-3-carboxylate (3)**
Organoboranes:
**4-(Methanesulfonyl)phenylboronic acid (4)**
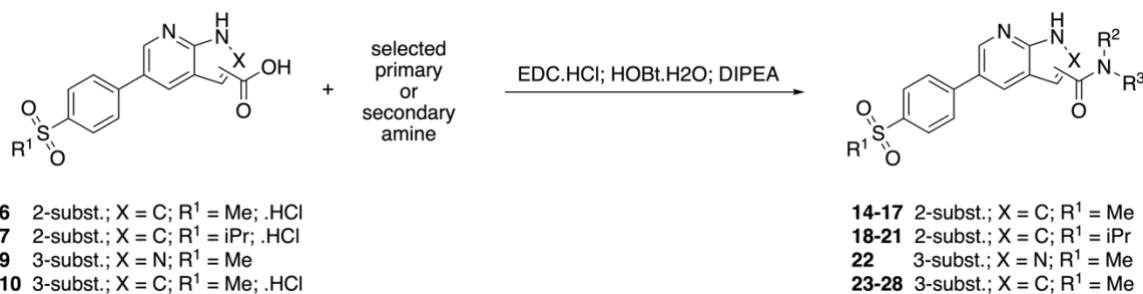**[4-(Propane-2-sulfonyl)phenyl]boronic acid (5)**

Products:

**5-(4-methanesulfonylphenyl)-1*H*-pyrrolo[2,3-b]pyridine-2-carboxylic acid hydrochloride (6):** Compound **1** (407 mg; 1.6 mmol); boronic acid **4** (416 mg; 2.1 mmol); $Na_2CO_3$ (1.70 g; 16.0 mmol) in 5.3 mL $H_2O$; Pd(dppf)$Cl_2$.DCM (13 mg; 0.016 mmol); and 30 mL anhydrous 1,4-dioxane. Brownish powder **6** with yield 56%.

$^1$H NMR (600 MHz, DMSO-$d_6$) δ 12.55 (s, 1H), 8.79 (s, 1H), 8.49 (s, 1H), 8.02 (s, 4H), 7.19 (s, 1H), 3.27 (s, 3H). $^{13}$C NMR (151 MHz, DMSO-$d_6$) δ 162.84, 149.19, 145.99, 144.03, 139.85, 130.77, 129.70, 128.23, 128.20, 127.96, 119.80, 107.14, 44.16. HRMS (ESI$^+$): [M+H]$^+$: calculated for $C_{15}H_{13}N_2O_4S^+$ (m/z): 317.05905; detected: 317.05948.

**5-[4-(propane-2-sulfonyl)phenyl]-1*H*-pyrrolo[2,3-b]pyridine-2-carboxylic acid hydrochloride (7):** Compound **1** (431 mg; 1.7 mmol); boronic acid **5** (504 mg; 2.21 mmol); $Na_2CO_3$ (1.79 g; 16.9 mmol) in 5.6 mL $H_2O$; Pd(dppf)$Cl_2$.DCM (14 mg; 0.017 mmol); and 30 mL anhydrous 1,4-dioxane. Brownish powder **7** with yield 96%.

$^1$H NMR (500 MHz, DMSO-$d_6$) δ 12.58 – 12.54 (m, 1H), 8.82 (s, 1H), 8.51 (d, $J$ = 2.3 Hz, 1H), 8.05 (d, $J$ = 8.3 Hz, 2H), 7.95 (d, $J$ = 8.3 Hz, 2H), 7.21 (d, $J$ = 2.0 Hz, 1H), 3.47 (p, $J$ = 6.8 Hz, 1H), 1.21 (d, $J$ = 6.7 Hz, 6H). $^{13}$C NMR (126 MHz, DMSO) δ 162.81, 149.19, 145.99, 144.16, 135.70, 130.67, 129.81, 129.63, 128.04, 127.80, 119.71, 107.10, 54.67, 15.71. HRMS (ESI$^+$): [M+H]$^+$: calculated for $C_{17}H_{17}N_2O_4S^+$ (m/z): 345.09035; detected: 345.09070.

**Methyl-5-(4-methanesulfonylphenyl)-1*H*-pyrrolo[2,3-b]pyridine-3-carboxylate (8):** Compound **2** (470 mg; 1.84 mmol); boronic acid **4** (480 mg; 2.4 mmol); $Na_2CO_3$ (1.95 g; 18.4 mmol) in 6.1 mL $H_2O$; Pd(dppf)$Cl_2$.DCM (15 mg; 0.018 mmol); and 30 mL anhydrous 1,4-dioxane.

Dark brown solid **8** was used in next step hydrolysis without NMR characterization, counting with quantitative yields. HRMS (ESI$^+$): [M+H]$^+$: calculated for $C_{16}H_{15}N_2O_4S^+$ (m/z): 331.07470; detected: 331.07428.

**5-(4-methanesulfonylphenyl)-1*H*-pyrazolo[3,4-b]pyridine-3-carboxylic acid (9):** Compound **3** (437 mg; 1.7 mmol); boronic acid **4** (442 mg; 2.21 mmol); $Na_2CO_3$ (1.80 g; 17.0 mmol) in 5.6 mL $H_2O$; Pd(dppf)Cl$_2$.DCM (14 mg; 0.017 mmol); and 30 mL anhydrous 1,4-dioxane. Dark brown powder **9** with yield 86%.

$^1$H NMR (600 MHz, DMSO-$d_6$) δ 9.01 (d, *J* = 2.1 Hz, 1H), 8.68 (d, *J* = 2.2 Hz, 1H), 8.11 – 8.04 (m, 4H), 3.28 (s, 3H). HRMS (ESI$^+$): [M+H]$^+$: calculated for $C_{14}H_{12}N_3O_4S^+$ (m/z): 318.05430; detected: 318.05396.

## 5.2.2 General procedure B: Hydrolysis of ester compounds
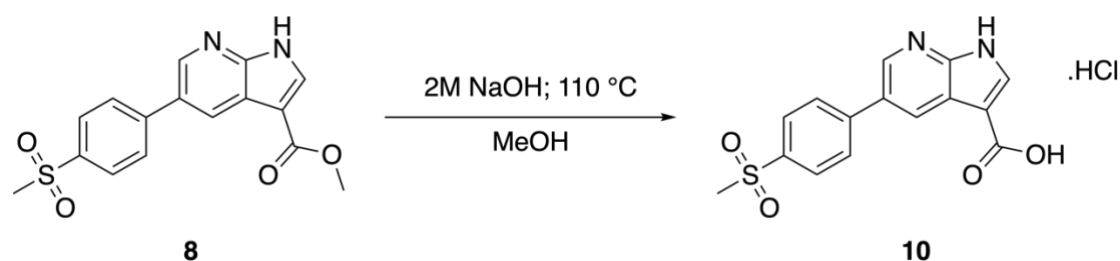


To a stirred solution of **8** in methanol (MeOH), 10% solution of NaOH was added and the mixture was heated to 110 °C overnight until reaction completion monitored by TLC. MeOH was removed by rotary evaporator and aqueous phase of carboxylic acid **10** was three times washed by EA (3x 100 mL) and then three times washed by DCM (3x 100 mL). Resulting aqueous phases were carefully acidified by 10% hydrochloric acid (HCl) to pH ≈ 1. Precipitates were filtered and washed by additional $H_2O$ (3x 20 mL) and then by hexane (3x 20 mL) to get product **10** as hydrochloric salt.

**5-(4-methanesulfonylphenyl)-1*H*-pyrrolo[2,3-b]pyridine-3-carboxylic acid hydrochloride (10):**

Compound **8** (607 mg; 1.84 mmol) was dissolved in 20 mL MeOH and 20 mL of 10% NaOH was added. Brown solid **10** with yield 88% after two steps.

$^1$H NMR (600 MHz, DMSO-$d_6$) δ 12.60 (d, *J* = 3.0 Hz, 1H), 8.70 (d, *J* = 2.3 Hz, 1H), 8.58 (d, *J* = 2.3 Hz, 1H), 8.23 (d, *J* = 2.9 Hz, 1H), 8.06 – 8.01 (m, 4H), 3.26 (s, 3H). $^{13}$C NMR (151 MHz, DMSO-$D_6$) δ 165.81, 149.28, 144.17, 143.51, 139.96, 134.47,

128.94, 128.40, 128.33, 127.73, 118.97, 107.34, 44.18. HRMS (ESI$^+$): [M+H]$^+$: calculated for $C_{15}H_{13}N_2O_4S^+$ (m/z): 317.05905; detected: 317.05865.

## 5.2.3 General procedure C: EDC catalyzed amide bond formation



**6** 2-subst.; X = C; R$^1$ = Me; .HCl
**7** 2-subst.; X = C; R$^1$ = iPr; .HCl
**9** 3-subst.; X = N; R$^1$ = Me
**10** 3-subst.; X = C; R$^1$ = Me; .HCl

**14-17** 2-subst.; X = C; R$^1$ = Me
**18-21** 2-subst.; X = C; R$^1$ = iPr
**22** 3-subst.; X = N; R$^1$ = Me
**23-28** 3-subst.; X = C; R$^1$ = Me

To a stirred solution of carboxylic acids **6**, **7**, **9**, or **10** (1.0 eq) in anhydrous tetrahydrofuran (THF) under Ar, *N*-(3-dimethylaminopropyl)-*N'*-ethylcarbodiimide hydrochloride (EDC.HCl; 1.0 eq) and 1-hydroxybenzotriazole hydrate (HOBt.H$_2$O; 1.1 eq) were subsequently added. *N*,*N*-diisopropylethylamine (DIPEA; 3.0 eq) was dropwise added and finally selected primary or secondary amine (1.0 eq) was introduced. The reaction mixture was stirred overnight (16 hours). After completion monitored by TLC, mixture was diluted by H$_2$O, the organic phase was removed, and water phase was extracted with EA (3x 30 mL). The combined organic phases were dried over Na$_2$SO$_4$, filtered, concentrated. The resulting residue was purified by column chromatography to obtain desired amide product, or MeOH was directly added for its precipitation.
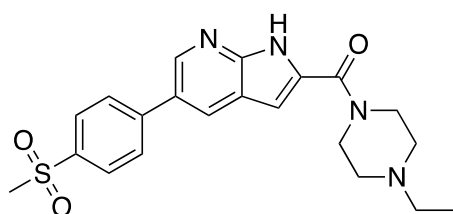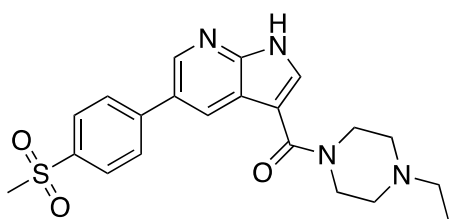


**1-ethyl-4-[5-(4-methanesulfonylphenyl)-1*H*-pyrrolo[2,3-b]pyridine-2-carbonyl]piperazine (14)**

Carboxylic acid **6** (110 mg; 0.312 mmol); EDC.HCl (60 mg; 0.312 mmol); HOBt.H$_2$O (53 mg; 0.343 mmol); DIPEA (163 μL; 0.936 mmol) and 1-ethylpiperazine (40 μL; 0.312 mmol) in 5 mL anhydrous THF. After extraction,

the residue was purified by column chromatography using mobile phase DCM/MeOH/NH$_4$OH (25% aqueous solution) (15:1:0.1) to get pure product **14** as light brownish solid. Yield 60%.

$^1$H NMR (600 MHz, DMSO-$d_6$) δ 12.32 (s, 1H), 8.71 (s, 1H), 8.40 (s, 1H), 8.04 – 7.97 (m, 4H), 6.81 (s, 1H), 3.75 – 3.64 (m, 4H), 3.27 (s, 3H), 2.47 – 2.40 (m, 4H), 2.37 (q, $J$ = 7.2 Hz, 2H), 1.03 (t, $J$ = 7.2 Hz, 3H). $^{13}$C NMR (151 MHz, DMSO-$D_6$) δ 161.47, 148.00, 143.99, 143.74, 139.18, 132.15, 128.09, 127.67, 127.60, 127.18, 119.00, 102.47, 52.36, 51.46, 43.61, 11.86. HRMS (ESI$^+$): [M+H]$^+$: calculated for C$_{21}$H$_{25}$N$_4$O$_3$S$^+$ (m/z): 413.16419; detected: 413.16434. LC-MS purity >99%
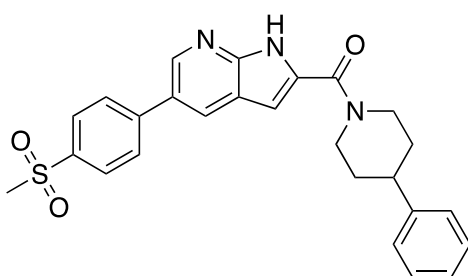


**1-[5-(4-methanesulfonylphenyl)-1$H$-pyrrolo[2,3-b]pyridine-2-carbonyl]-4-phenylpiperidine (15)**

Carboxylic acid **6** (97 mg; 0.275 mmol); EDC.HCl (53 mg; 0.275 mmol); HOBt.H$_2$O (46 mg; 0.302 mmol); DIPEA (144 µL; 0.825 mmol) and 4-phenylpiperidine (44 mg; 0.275 mmol) in 5 mL anhydrous THF. After extraction, the residue was purified by column chromatography using mobile phase DCM/EA (1:1) to get pure product **15** as white solid. Yield 28%.

$^1$H NMR (600 MHz, DMSO-$d_6$) δ 12.33 (s, 1H), 8.71 (d, $J$ = 2.2 Hz, 1H), 8.40 (d, $J$ = 2.2 Hz, 1H), 8.02 (s, 4H), 7.39 – 7.24 (m, 4H), 7.22 – 7.16 (m, 1H), 6.85 (s, 1H), 4.83 – 4.16 (m, 2H), 3.27 (s, 3H), 3.21 – 2.93 (m, 2H), 2.93 – 2.83 (m, 1H), 1.94 – 1.81 (m, 2H), 1.74 – 1.60 (m, 2H). $^{13}$C NMR (151 MHz, DMSO-$D_6$) δ 162.16, 148.58, 146.06, 144.41, 144.34, 139.73, 133.14, 128.98, 128.58, 128.23, 128.16, 127.73, 127.30, 126.81, 119.63, 102.60, 44.16, 42.33, 33.62. HRMS (ESI$^+$): [M+H]$^+$: calculated for C$_{26}$H$_{26}$N$_3$O$_3$S$^+$ (m/z): 460.16894; detected: 460.16803. LC-MS purity 98%
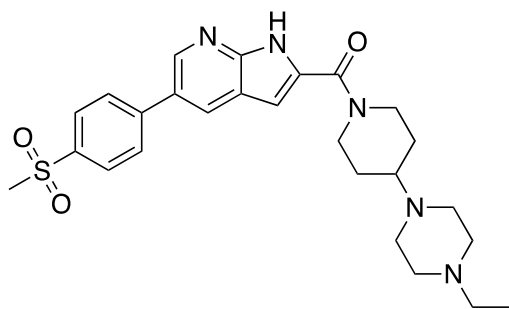
**1-ethyl-4-{1-[5-(4-methanesulfonylphenyl)-1H-pyrrolo[2,3-b]pyridine-2-carbonyl]piperidin-4-yl}piperazine (16)**

Carboxylic acid **6** (97 mg; 0.275 mmol); EDC.HCl (53 mg; 0.275 mmol); HOBt.H₂O (46 mg; 0.302 mmol); DIPEA (144 µL; 0.825 mmol) and 1-ethyl-4-(piperidin-4-yl)piperazine (55 mg; 0.275 mmol) in 5 mL anhydrous THF. After extraction, the residue was purified by column chromatography using mobile phase DCM/MeOH/NH₄OH (25% aqueous solution) (15:1:0.1) to get pure product **16** as light brownish solid. Yield 52%.

$^1$H NMR (600 MHz, DMSO-$d_6$) δ 12.30 (s, 1H), 8.70 (d, $J$ = 2.2 Hz, 1H), 8.39 (d, $J$ = 2.3 Hz, 1H), 8.01 (s, 4H), 6.80 (s, 1H), 4.33 (s, 2H), 3.36 – 3.30 (m, 2H), 3.27 (s, 3H), 2.51 – 2.32 (m, 9H), 2.28 (q, $J$ = 7.2 Hz, 2H), 1.87 – 1.79 (m, 2H), 1.48 – 1.39 (m, 2H), 0.97 (t, $J$ = 7.2 Hz, 3H). $^{13}$C NMR (151 MHz, DMSO-$D_6$) δ 162.00, 148.55, 144.41, 144.33, 139.73, 133.04, 128.57, 128.23, 128.15, 127.71, 119.60, 102.58, 61.21, 53.35, 52.17, 49.12, 44.17, 28.61, 12.52. HRMS (ESI⁺): [M+H]⁺: calculated for C₂₆H₃₄N₅O₃S⁺ (m/z): 496.23769; detected: 496.23700. LC-MS purity >99%
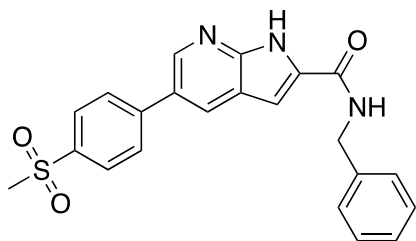


**N-benzyl-5-(4-methanesulfonylphenyl)-1H-pyrrolo[2,3-b]pyridine-2-carboxamide (17)**

Carboxylic acid **6** (120 mg; 0.340 mmol); EDC.HCl (65 mg; 0.275 mmol); HOBt.H₂O (57 mg; 0.374 mmol); DIPEA (195 µL; 1.12 mmol) and benzylamine (37 µL; 0.340 mmol) in 5 mL anhydrous THF. After extraction, the residue was

purified by column chromatography using mobile phase DCM/EA (1:1). The purified residue was additionally precipitated in MeOH and filtered to get pure product **17** as white solid. Yield 53%.

$^1$H NMR (500 MHz, DMSO-$d_6$) δ 12.34 (s, 1H), 9.17 (t, $J$ = 6.0 Hz, 1H), 8.74 (d, $J$ = 2.3 Hz, 1H), 8.49 (d, $J$ = 2.3 Hz, 1H), 8.08 – 7.99 (m, 4H), 7.40 – 7.32 (m, 4H), 7.30 – 7.23 (m, 2H), 4.54 (d, $J$ = 5.9 Hz, 2H), 3.27 (s, 3H). $^{13}$C NMR (126 MHz, DMSO) δ 160.93, 148.86, 144.99, 144.16, 139.84, 139.66, 133.82, 129.07, 128.84, 128.12, 128.10, 127.82, 127.67, 127.37, 119.88, 102.70, 44.10, 42.80. HRMS (ESI$^+$): [M+H]$^+$: calculated for $C_{22}H_{20}N_3O_3S^+$ (m/z): 406.12199; detected: 406.12167. LC-MS purity 97%



**1-ethyl-4-[5-(4-methanesulfonylphenyl)-1*H*-pyrrolo[2,3-b]pyridine-3-carbonyl]piperazine (18)**

Carboxylic acid **10** (86 mg; 0.244 mmol); EDC.HCl (47 mg; 0.244 mmol); HOBt.H$_2$O (41 mg; 0.268 mmol); DIPEA (127 µL; 0.731 mmol) and 1-ethylpiperazine (31 µL; 0.244 mmol) in 5 mL anhydrous THF. After extraction, the residue was purified by column chromatography using mobile phase DCM/MeOH/NH$_4$OH (25% aqueous solution) (15:1:0.1) to get pure product **18** as light brownish solid. Yield 25%.

$^1$H NMR (600 MHz, CD$_3$OD-$d_4$) δ 8.63 (d, $J$ = 2.2 Hz, 1H), 8.45 (d, $J$ = 2.2 Hz, 1H), 8.09 – 8.01 (m, 2H), 7.99 – 7.92 (m, 2H), 7.87 (s, 1H), 3.93 – 3.80 (m, 4H), 3.17 (s, 3H), 2.61 (t, $J$ = 5.2 Hz, 4H), 2.54 (q, $J$ = 7.3 Hz, 2H), 1.15 (t, $J$ = 7.2 Hz, 3H). $^{13}$C NMR (151 MHz, CD$_3$OD -$D_4$) δ 165.99, 147.92, 144.48, 142.83, 139.45, 129.53, 128.87, 127.89, 127.82, 119.25, 108.81, 62.99, 52.45, 51.88, 43.12, 10.38. HRMS (ESI$^+$): [M+H]$^+$: calculated for $C_{21}H_{25}N_4O_3S^+$ (m/z): 413.16419; detected: 413.16357. LC-MS purity 99%
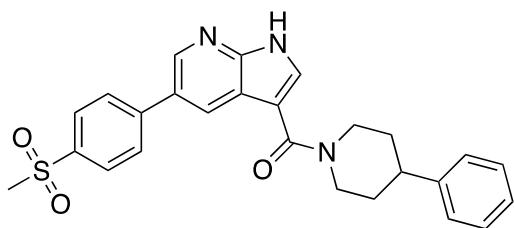
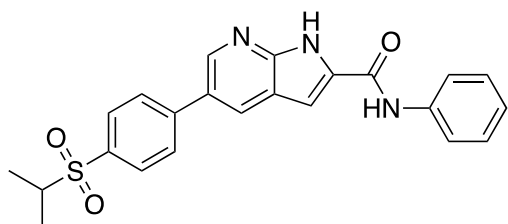**1-[5-(4-methanesulfonylphenyl)-1*H*-pyrrolo[2,3-b]pyridine-3-carbonyl]-4-phenylpiperidine (19)**

Carboxylic acid **10** (85 mg; 0.242 mmol); EDC.HCl (46 mg; 0.242 mmol); HOBt.H$_2$O (41 mg; 0.266 mmol); DIPEA (126 µL; 0.725 mmol) and 4-phenylpiperidine (39 mg; 0.242 mmol) in 5 mL anhydrous THF. After extraction, the residue was purified by column chromatography using mobile phase DCM/EA (1:1). The purified residue was additionally precipitated in MeOH and filtered to get pure product **19** as white solid. Yield 32%.

$^1$H NMR (500 MHz, DMSO-$d_6$) δ 12.35 (s, 1H), 8.69 (d, *J* = 2.2 Hz, 1H), 8.42 (d, *J* = 2.3 Hz, 1H), 8.03 (s, 4H), 7.96 (d, *J* = 1.7 Hz, 1H), 7.34 – 7.27 (m, 4H), 7.23 – 7.16 (m, 1H), 4.51 – 4.46 (m, 2H), 3.27 (s, 3H), 3.19 – 3.04 (m, 1H), 2.88 – 2.79 (m, 1H), 1.88 – 1.81 (m, 2H), 1.72 – 1.60 (m, 2H). $^{13}$C NMR (126 MHz, DMSO) δ 164.64, 148.57, 146.19, 144.21, 143.19, 139.74, 129.79, 128.88, 128.22, 128.18, 127.99, 127.57, 127.25, 126.67, 119.25, 109.79, 44.10, 42.48, 33.71. HRMS (ESI$^+$): [M+H]$^+$: calculated for C$_{26}$H$_{26}$N$_3$O$_3$S$^+$ (m/z): 460.16894; detected: 460.16849. LC-MS purity 98%
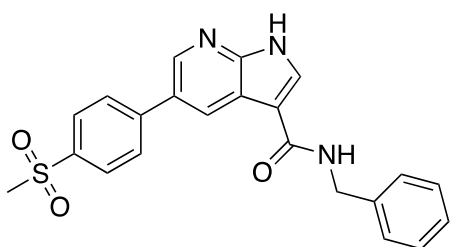


**_N_-benzyl-5-(4-methanesulfonylphenyl)-1*H*-pyrrolo[2,3-b]pyridine-3-carboxamide (20)**

Carboxylic acid **10** (94 mg; 0.266 mmol); EDC.HCl (51 mg; 0.266 mmol); HOBt.H$_2$O (45 mg; 0.293 mmol); DIPEA (139 µL; 0.800 mmol) and benzylamine (25 µL; 0.266 mmol) in 5 mL anhydrous THF. After extraction, the residue was purified by column chromatography using mobile phase DCM/EA (1:1). The purified residue was additionally precipitated in MeOH and filtered to get pure product **20** as white solid. Yield 23%.

$^1$H NMR (500 MHz, DMSO-$d_6$) δ 12.31 (s, 1H), 8.79 (d, $J$ = 2.3 Hz, 1H), 8.70 – 8.63 (m, 2H), 8.29 (s, 1H), 8.06 – 7.98 (m, 4H), 7.39 – 7.29 (m, 4H), 7.28 – 7.21 (m, 1H), 4.52 (d, $J$ = 5.9 Hz, 2H), 3.27 (s, 3H). $^{13}$C NMR (126 MHz, DMSO) δ 164.21, 148.95, 144.30, 143.20, 140.63, 139.75, 129.95, 128.76, 128.28, 128.23, 128.19, 128.14, 127.71, 127.15, 119.00, 110.25, 44.11, 42.40. HRMS (ESI$^+$): [M+H]$^+$: calculated for $C_{22}H_{20}N_3O_3S^+$ (m/z): 406.12199; detected: 406.12073. LC-MS purity 96%
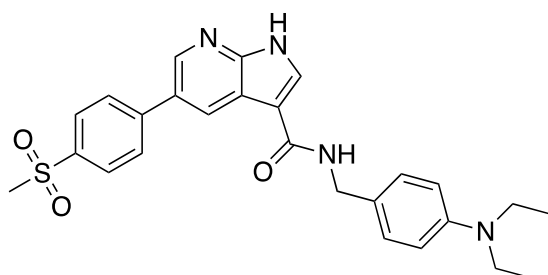


**N-{[4-(diethylamino)phenyl]methyl}-5-(4-methanesulfonylphenyl)-1H-pyrrolo[2,3-b]pyridine-3-carboxamide (21)**

Carboxylic acid **10** (107 mg; 0.303 mmol); EDC.HCl (58 mg; 0.303 mmol); HOBt.H$_2$O (51 mg; 0.334 mmol); DIPEA (158 µL; 0.910 mmol) and (4-aminomethylphenyl)diethylamine (55 µL; 0.303 mmol) in 5 mL anhydrous THF. After extraction, the residue was purified by column chromatography using mobile phase DCM/EA (1:1) to get pure product **21** as white solid. Yield 21%.

$^1$H NMR (500 MHz, DMSO-$d_6$) δ 12.27 (s, 1H), 8.79 (d, $J$ = 2.3 Hz, 1H), 8.67 (d, $J$ = 2.3 Hz, 1H), 8.47 (t, $J$ = 5.9 Hz, 1H), 8.26 (s, 1H), 8.08 – 7.96 (m, 4H), 7.19 – 7.08 (m, 2H), 6.65 – 6.56 (m, 2H), 4.36 (d, $J$ = 5.9 Hz, 2H), 3.30 (q, $J$ = 7.0 Hz, 4H), 3.27 (s, 3H), 1.05 (t, $J$ = 7.0 Hz, 6H). $^{13}$C NMR (126 MHz, DMSO) δ 163.98, 148.93, 146.89, 144.33, 143.12, 139.73, 129.74, 129.14, 128.23, 128.21, 128.18, 126.77, 119.06, 112.07, 110.46, 44.17, 44.11, 42.00, 12.85. HRMS (ESI$^+$): [M+H]$^+$: calculated for $C_{26}H_{29}N_4O_3S^+$ (m/z): 477.19549; detected: 477.19504. LC-MS purity 98%
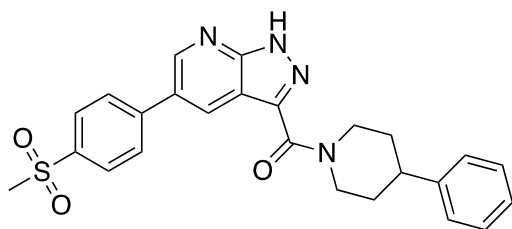
**1-[5-(4-methanesulfonylphenyl)-1*H*-pyrazolo[3,4-b]pyridine-3-carbonyl]-4-phenylpiperidine (22)**

Carboxylic acid **9** (109 mg; 0.308 mmol); EDC.HCl (59 mg; 0.308 mmol); HOBt.$H_2O$ (52 mg; 0.339 mmol); DIPEA (161 µL; 0.924 mmol) and 4-phenylpiperidine (50 mg; 0.308 mmol) in 5 mL anhydrous THF. After extraction, the residue was directly precipitated in MeOH and filtered to get pure product **22** as white solid. Yield 46%.

$^1$H NMR (500 MHz, DMSO-$d_6$) δ 14.25 (s, 1H), 9.00 (d, *J* = 2.3 Hz, 1H), 8.71 (d, *J* = 2.3 Hz, 1H), 8.07 (q, *J* = 8.3 Hz, 4H), 7.34 – 7.25 (m, 4H), 7.20 (t, *J* = 6.9 Hz, 1H), 5.03 – 4.96 (m, 1H), 4.81 – 4.75 (m, 1H), 3.29 (s, 3H), 3.01 – 2.85 (m, 2H), 1.99 – 1.81 (m, 2H), 1.75 – 1.64 (m, 2H). $^{13}$C NMR (126 MHz, DMSO) δ 161.38, 152.12, 149.50, 146.05, 143.11, 140.28, 139.82, 129.81, 129.35, 128.91, 128.53, 128.24, 127.24, 126.70, 115.37, 47.25, 44.03, 43.07, 42.38, 34.22, 33.34. HRMS (ESI$^+$): [M+H]$^+$: calculated for $C_{25}H_{25}N_4O_3S^+$ (m/z): 461.16419; detected: 461.16458. LC-MS purity 98%
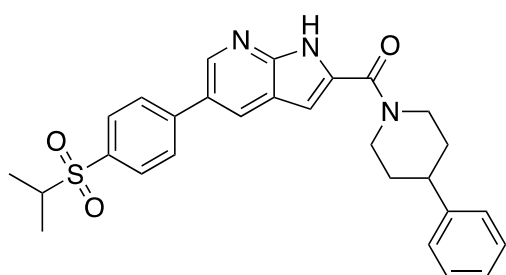


**1-{5-[4-(propane-2-sulfonyl)phenyl]-1*H*-pyrrolo[2,3-b]pyridine-2-carbonyl}-4-phenylpiperidine (23)**

Carboxylic acid **7** (99 mg; 0.260 mmol); EDC.HCl (50 mg; 0.260 mmol); HOBt.$H_2O$ (44 mg; 0.286 mmol); DIPEA (136 µL; 0.780 mmol) and 4-phenylpiperidine (42 mg; 0.260 mmol) in 5 mL anhydrous THF. After extraction, the residue was directly precipitated in MeOH and filtered to get pure product **23** as white solid. Yield 70%.

$^1$H NMR (500 MHz, DMSO-$d_6$) δ 12.34 (s, 1H), 8.73 (d, $J$ = 2.2 Hz, 1H), 8.42 (d, $J$ = 2.4 Hz, 1H), 8.03 (d, $J$ = 8.1 Hz, 2H), 7.94 (d, $J$ = 8.1 Hz, 2H), 7.36 – 7.25 (m, 3H), 7.21 (t, $J$ = 7.0 Hz, 1H), 6.85 (d, $J$ = 2.0 Hz, 1H), 4.82 – 4.19 (m, 2H), 3.52 – 3.42 (m, $J$ = 6.9, 6.4 Hz, 1H), 3.27 – 2.94 (m, 2H), 2.92 – 2.82 (m, 1H), 1.90 – 1.84 (m, 2H), 1.74 – 1.65 (m, 2H), 1.20 (d, $J$ = 6.8 Hz, 6H). $^{13}$C NMR (126 MHz, DMSO) δ 162.07, 148.53, 145.99, 144.44, 144.37, 135.59, 133.06, 129.82, 128.91, 128.55, 128.00, 127.53, 127.23, 126.74, 119.56, 102.57, 54.67, 42.26, 33.56, 15.73. HRMS (ESI$^+$): [M+H]$^+$: calculated for $C_{28}H_{30}N_3O_3S^+$ (m/z): 488.20024; detected: 488.19946. LC-MS purity 95%
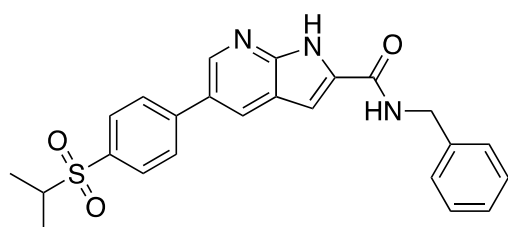


**$N$-benzyl-5-[4-(propane-2-sulfonyl)phenyl]-1$H$-pyrrolo[2,3-b]pyridine-2-carboxamide (24)**

Carboxylic acid **7** (99 mg; 0.260 mmol); EDC.HCl (50 mg; 0.260 mmol); HOBt.H$_2$O (44 mg; 0.286 mmol); DIPEA (136 μL; 0.780 mmol) and benzylamine (28 μL; 0.260 mmol) in 5 mL anhydrous THF. After extraction, the residue was directly precipitated in MeOH and filtered to get pure product **24** as white solid. Yield 73%.
$^1$H NMR (500 MHz, DMSO-$d_6$) δ 12.35 (s, 1H), 9.16 (t, $J$ = 6.0 Hz, 1H), 8.75 (d, $J$ = 2.2 Hz, 1H), 8.50 (d, $J$ = 2.3 Hz, 1H), 8.08 – 8.02 (m, 2H), 7.96 – 7.91 (m, 2H), 7.40 – 7.32 (m, 4H), 7.30 – 7.23 (m, 2H), 4.54 (d, $J$ = 5.9 Hz, 2H), 3.46 (hept, $J$ = 6.9 Hz, 1H), 1.19 (d, $J$ = 6.8 Hz, 6H). $^{13}$C NMR (126 MHz, DMSO) δ 160.93, 148.88, 145.00, 144.35, 139.84, 135.58, 133.82, 129.77, 129.13, 128.84, 128.02, 127.82, 127.56, 127.37, 119.88, 102.72, 54.68, 42.80, 15.72. HRMS (ESI$^+$): [M+H]$^+$: calculated for $C_{24}H_{24}N_3O_3S^+$ (m/z): 434.15329; detected: 434.15277. LC-MS purity 96%

**N-phenyl-5-[4-(propane-2-sulfonyl)phenyl]-1H-pyrrolo[2,3-b]pyridine-2-carboxamide (25)**

Carboxylic acid **7** (105 mg; 0.276 mmol); EDC.HCl (53 mg; 0.276 mmol); HOBt.H$_2$O (46 mg; 0.303 mmol); DIPEA (144 µL; 0.827 mmol) and aniline (25 µL; 0.276 mmol) in 5 mL anhydrous THF. After extraction, the residue was directly precipitated in MeOH and filtered to get pure product **25** as white solid. Yield 68%.

$^1$H NMR (500 MHz, DMSO-$d_6$) δ 12.51 (d, J = 2.1 Hz, 1H), 10.34 (s, 1H), 8.79 (d, J = 2.3 Hz, 1H), 8.56 (d, J = 2.3 Hz, 1H), 8.10 – 8.03 (m, 2H), 7.98 – 7.90 (m, 2H), 7.85 – 7.79 (m, 2H), 7.51 (d, J = 2.0 Hz, 1H), 7.43 – 7.35 (m, 2H), 7.17 – 7.10 (m, 1H), 3.47 (hept, J = 6.8 Hz, 1H), 1.20 (d, J = 6.7 Hz, 6H). $^{13}$C NMR (126 MHz, DMSO) δ 159.52, 149.06, 145.46, 144.28, 139.23, 135.65, 133.70, 129.79, 129.38, 129.24, 128.07, 127.76, 124.28, 120.65, 119.82, 103.90, 54.69, 15.73. HRMS (ESI$^+$): [M+H]$^+$: calculated for C$_{23}$H$_{22}$N$_3$O$_3$S$^+$ (m/z): 420.13764; detected: 420.13632. LC-MS purity 98%
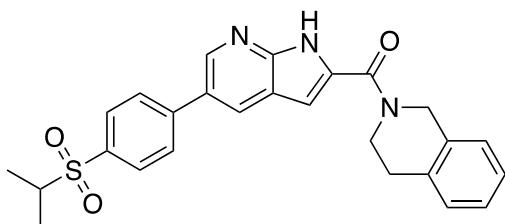


**2-{5-[4-(propane-2-sulfonyl)phenyl]-1H-pyrrolo[2,3-b]pyridine-2-carbonyl}-1,2,3,4-tetrahydroisoquinoline (26)**

Carboxylic acid **7** (105 mg; 0.276 mmol); EDC.HCl (53 mg; 0.276 mmol); HOBt.H$_2$O (46 mg; 0.303 mmol); DIPEA (144 µL; 0.827 mmol) and 1,2,3,4-tetrahydroisoquinoline (35 µL; 0.276 mmol) in 5 mL anhydrous THF. After extraction, the residue was directly precipitated in MeOH and filtered to get pure product **26** as white solid. Yield 58%.

$^1$H NMR (500 MHz, DMSO-$d_6$) δ 12.39 (s, 1H), 8.75 (d, J = 2.3 Hz, 1H), 8.45 (d, J = 2.3 Hz, 1H), 8.04 (d, J = 8.4 Hz, 2H), 7.94 (d, J = 8.2 Hz, 2H), 7.23 – 7.17 (m, 4H), 6.96 (s, 1H), 4.86 (s, 2H), 3.93 (s, 2H), 3.47 (hept, J = 6.8 Hz, 1H), 2.98 – 2.92 (m, 2H), 1.20 (d, J = 6.8 Hz, 6H). $^{13}$C NMR (126 MHz, DMSO) δ 148.56, 144.70, 144.41, 135.62, 135.07, 133.59, 132.75, 129.82, 129.00, 128.79, 128.02, 127.59, 127.10, 126.76, 119.58, 54.67, 15.73. HRMS (ESI$^+$): [M+H]$^+$: calculated for C$_{26}$H$_{26}$N$_3$O$_3$S$^+$ (m/z): 460.16894; detected: 460.16739. LC-MS purity 98%
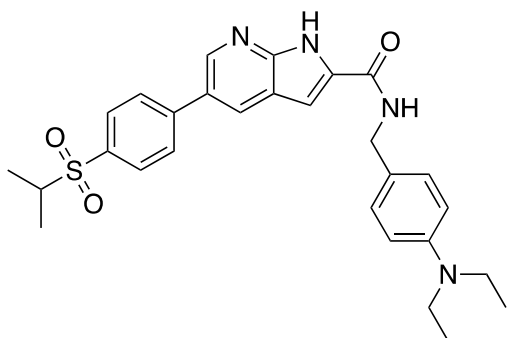
**N-{[4-(diethylamino)phenyl]methyl}-5-[4-(propane-2-sulfonyl)phenyl]-1H-pyrrolo[2,3-b]pyridine-2-carboxamide (27)**

Carboxylic acid **7** (92 mg; 0.242 mmol); EDC.HCl (46 mg; 0.242 mmol); HOBt.H₂O (41 mg; 0.266 mmol); DIPEA (126 µL; 0.725 mmol) and (4-aminomethylphenyl)diethylamine (44 µL; 0.242 mmol) in 5 mL anhydrous THF. After extraction, the residue was purified by column chromatography using mobile phase DCM/EA (1:1) to get pure product **27** as light orange solid. Yield 25%

$^1$H NMR (500 MHz, DMSO-$d_6$) δ 12.29 (s, 1H), 8.95 (t, $J$ = 5.9 Hz, 1H), 8.73 (d, $J$ = 2.2 Hz, 1H), 8.47 (d, $J$ = 2.3 Hz, 1H), 8.07 – 8.01 (m, 2H), 7.95 – 7.89 (m, 2H), 7.24 (s, 1H), 7.18 – 7.10 (m, 2H), 6.65 – 6.59 (m, 2H), 4.37 (d, $J$ = 5.8 Hz, 2H), 3.45 (hept, $J$ = 6.8 Hz, 1H), 3.29 (q, $J$ = 7.0 Hz, 4H), 1.19 (d, $J$ = 6.8 Hz, 6H), 1.05 (t, $J$ = 7.0 Hz, 6H). $^{13}$C NMR (126 MHz, DMSO) δ 160.59, 148.84, 147.03, 144.88, 144.37, 135.56, 134.06, 129.76, 129.31, 129.05, 128.01, 127.51, 125.91, 119.89, 112.03, 102.61, 54.68, 44.16, 42.47, 15.72, 12.85. HRMS (ESI$^+$): [M+H]$^+$: calculated for C$_{28}$H$_{33}$N$_4$O$_3$S$^+$ (m/z): 505.22679; detected: 505.22714. LC-MS purity 98%
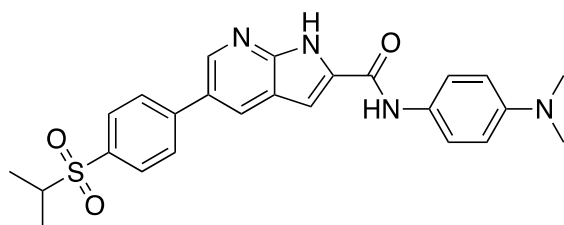


**N-[4-(dimethylamino)phenyl]-5-[4-(propane-2-sulfonyl)phenyl]-1H-pyrrolo[2,3-b]pyridine-2-carboxamide (28)**

Carboxylic acid **7** (92 mg; 0.242 mmol); EDC.HCl (46 mg; 0.242 mmol); HOBt.H₂O (41 mg; 0.266 mmol); DIPEA (126 µL; 0.725 mmol) and *N,N*-dimethyl-*p*-

phenylenediamine (33 mg; 0.242 mmol) in 5 mL anhydrous THF. After extraction, the residue was directly precipitated in MeOH, filtered, and washed by cold acetone to get pure product **28** as light green solid. Yield 20%

$^1$H NMR (500 MHz, DMSO-$d_6$) δ 12.40 (s, 1H), 10.11 (s, 1H), 8.77 (d, $J$ = 2.2 Hz, 1H), 8.53 (d, $J$ = 2.3 Hz, 1H), 8.07 (d, $J$ = 8.1 Hz, 2H), 7.94 (d, $J$ = 8.0 Hz, 2H), 7.61 (d, $J$ = 8.6 Hz, 2H), 7.43 (s, 1H), 6.76 (d, $J$ = 8.5 Hz, 2H), 3.47 (p, $J$ = 6.8 Hz, 1H), 2.89 (s, 6H), 1.20 (d, $J$ = 6.8 Hz, 6H). $^{13}$C NMR (126 MHz, DMSO) δ 158.84, 148.97, 147.89, 145.09, 144.35, 135.59, 134.20, 129.78, 129.14, 128.78, 128.05, 127.65, 122.10, 119.93, 113.01, 103.16, 54.69, 40.90, 15.73. HRMS (ESI$^+$): [M+H]$^+$: calculated for $C_{25}H_{27}N_4O_3S^+$ (m/z): 463.17984; detected: 463.17856. LC-MS purity 95%

# List of Figures

# List of Tables

# REFERENCES

(1) University of Edinburgh. Neoplasia – definition, nomenclature and spread – Pathologia https://pathologia.ed.ac.uk/topic/neoplasia-definition-nomenclature-and-spread/ (accessed 2022 -02 -21).

(2) Jordan, J. T.; Plotkin, S. R. Benign Intracranial Tumors. *Neurologic Clinics* **2018**, *36* (3), 501–516. https://doi.org/10.1016/j.ncl.2018.04.007.

(3) Klener Jr., P.; Klener, P. *Principy systémové protinádorové léčby*, 1st ed.; Grada: Praha, 2013; Vol. 1.

(4) Sung, H.; Ferlay, J.; Siegel, R. L.; Laversanne, M.; Soerjomataram, I.; Jemal, A.; Bray, F. Global Cancer Statistics 2020: GLOBOCAN Estimates of Incidence and Mortality Worldwide for 36 Cancers in 185 Countries. *CA: A Cancer Journal for Clinicians* **2021**, *71* (3), 209–249. https://doi.org/10.3322/caac.21660.

(5) Den boje proti rakovině a statistiky ÚZIS ČR - Aktuality - ÚZIS ČR https://www.uzis.cz/index.php?pg=aktuality&aid=8466 (accessed 2022 -03 -09).

(6) American Cancer Society Inc. Cancer Facts & Figures 2021 https://www.cancer.org/research/cancer-facts-statistics/all-cancer-facts-figures/cancer-facts-figures-2021.html (accessed 2022 -03 -29).

(7) ČOS ČLS JEP. Životní styl » Linkos.cz https://www.linkos.cz/onkologicka-prevence/zasady-zdraveho-zivotniho-stylu/ (accessed 2022 -03 -09).

(8) Rebbeck, T. R.; Burns-White, K.; Chan, A. T.; Emmons, K.; Freedman, M.; Hunter, D. J.; Kraft, P.; Laden, F.; Mucci, L.; Parmigiani, G.; Schrag, D.; Syngal, S.; Tamimi, R. M.; Viswanath, K.; Yurgelun, M. B.; Garber, J. E. Precision Prevention and Early Detection of Cancer: Fundamental Principles. *Cancer Discov* **2018**, *8* (7), 803–811. https://doi.org/10.1158/2159-8290.CD-17-1415.

(9) Lakdawalla, A.; Fisher, J.; Ronaghi, M.; Fan, J.-B. Cancer Genome Sequencing. In *Molecular Oncology: Causes of Cancer and Targets for Treatment*; Gelmann, E. P., Sawyers, C. L., Rauscher, III, F. J., Eds.; Cambridge University Press: Cambridge, 2013; pp 1–9. https://doi.org/10.1017/CBO9781139046947.002.

(10) Hanahan, D. Hallmarks of Cancer: New Dimensions. *Cancer Discov* **2022**, *12* (1), 31–46. https://doi.org/10.1158/2159-8290.CD-21-1059.

(11) Hanahan, D.; Weinberg, R. A. Hallmarks of Cancer: The Next Generation. *Cell* **2011**, *144* (5), 646–674. https://doi.org/10.1016/j.cell.2011.02.013.

(12) Hanahan, D.; Weinberg, R. A. The Hallmarks of Cancer. *Cell* **2000**, *100* (1), 57–70. https://doi.org/10.1016/S0092-8674(00)81683-9.

(13) Klaunig, J. E. Carcinogenesis. In *An Introduction to Interdisciplinary Toxicology*; Elsevier, 2020; pp 97–110. https://doi.org/10.1016/B978-0-12-813602-7.00008-9.

(14) Cha, H.-J.; Yim, H. The Accumulation of DNA Repair Defects Is the Molecular Origin of Carcinogenesis. *Tumor Biol.* **2013**, *34* (6), 3293–3302. https://doi.org/10.1007/s13277-013-1038-y.

(15) Ribezzo, F.; Shiloh, Y.; Schumacher, B. Systemic DNA Damage Responses in Aging and Diseases. *Seminars in Cancer Biology* **2016**, *37–38*, 26–35. https://doi.org/10.1016/j.semcancer.2015.12.005.

(16) Wang, M.; Chen, S.; Ao, D. Targeting DNA Repair Pathway in Cancer: Mechanisms and Clinical Application. *MedComm (2020)* **2021**, *2* (4), 654–691. https://doi.org/10.1002/mco2.103.

(17) Visser, H.; Thomas, A. D. MicroRNAs and the DNA Damage Response: How Is Cell Fate Determined? *DNA Repair* **2021**, *108*, 103245. https://doi.org/10.1016/j.dnarep.2021.103245.

(18) O'Connor, M. J. Targeting the DNA Damage Response in Cancer. *Molecular Cell* **2015**, *60* (4), 547–560. https://doi.org/10.1016/j.molcel.2015.10.040.

(19) Weber, A. M.; Ryan, A. J. ATM and ATR as Therapeutic Targets in Cancer. *Pharmacology & Therapeutics* **2015**, *149*, 124–138. https://doi.org/10.1016/j.pharmthera.2014.12.001.

(20) Gorecki, L.; Andrs, M.; Rezacova, M.; Korabecny, J. Discovery of ATR Kinase Inhibitor Berzosertib (VX-970, M6620): Clinical Candidate for Cancer Therapy. *Pharmacology & Therapeutics* **2020**, *210*, 107518. https://doi.org/10.1016/j.pharmthera.2020.107518.

(21) Topatana, W.; Juengpanich, S.; Li, S.; Cao, J.; Hu, J.; Lee, J.; Suliyanto, K.; Ma, D.; Zhang, B.; Chen, M.; Cai, X. Advances in Synthetic Lethality for Cancer Therapy: Cellular Mechanism and Clinical Translation. *Journal of*

*Hematology & Oncology* **2020**, *13* (1), 118. https://doi.org/10.1186/s13045-020-00956-5.

(22) Blackford, A. N.; Jackson, S. P. ATM, ATR, and DNA-PK: The Trinity at the Heart of the DNA Damage Response. *Molecular Cell* **2017**, *66* (6), 801–817. https://doi.org/10.1016/j.molcel.2017.05.015.

(23) Massagué, J. G1 Cell-Cycle Control and Cancer. *Nature* **2004**, *432* (7015), 298–306. https://doi.org/10.1038/nature03094.

(24) Andrs, M.; Korabecny, J.; Nepovimova, E.; Jun, D.; Hodny, Z.; Moravcova, S.; Hanzlikova, H.; Kuca, K. The Development of Ataxia Telangiectasia Mutated Kinase Inhibitors. *MRMC* **2014**, *14* (999), 1–1. https://doi.org/10.2174/1389557514666141013140217.

(25) Sundar, R.; Brown, J.; Ingles Russo, A.; Yap, T. A. Targeting ATR in Cancer Medicine. *Current Problems in Cancer* **2017**, *41* (4), 302–315. https://doi.org/10.1016/j.currproblcancer.2017.05.002.

(26) Cheng, B.; Pan, W.; Xing, Y.; Xiao, Y.; Chen, J.; Xu, Z. Recent Advances in DDR (DNA Damage Response) Inhibitors for Cancer Therapy. *European Journal of Medicinal Chemistry* **2022**, *230*, 114109. https://doi.org/10.1016/j.ejmech.2022.114109.

(27) Zheng, F.; Zhang, Y.; Chen, S.; Weng, X.; Rao, Y.; Fang, H. Mechanism and Current Progress of Poly ADP-Ribose Polymerase (PARP) Inhibitors in the Treatment of Ovarian Cancer. *Biomedicine & Pharmacotherapy* **2020**, *123*, 109661. https://doi.org/10.1016/j.biopha.2019.109661.

(28) Pires, I. M.; Olcina, M. M.; Anbalagan, S.; Pollard, J. R.; Reaper, P. M.; Charlton, P. A.; McKenna, W. G.; Hammond, E. M. Targeting Radiation-Resistant Hypoxic Tumour Cells through ATR Inhibition. *Br J Cancer* **2012**, *107* (2), 291–299. https://doi.org/10.1038/bjc.2012.265.

(29) National Library of Medicine (US). ClinicalTrials.gov https://clinicaltrials.gov/ct2/home (accessed 2022 -03 -29).

(30) Karnitz, L. M.; Zou, L. Molecular Pathways: Targeting ATR in Cancer Therapy. *Clinical Cancer Research* **2015**, *21* (21), 4780–4785. https://doi.org/10.1158/1078-0432.CCR-15-0479.

(31) Knegtel, R.; Charrier, J.-D.; Durrant, S.; Davis, C.; O'Donnell, M.; Storck, P.; MacCormick, S.; Kay, D.; Pinder, J.; Virani, A.; Twin, H.; Griffiths, M.; Reaper, P.; Littlewood, P.; Young, S.; Golec, J.; Pollard, J. Rational Design of 5-(4-

(Isopropylsulfonyl)Phenyl)-3-(3-(4-((Methylamino)Methyl)Phenyl)Isoxazol-5-Yl)Pyrazin-2-Amine (VX-970, M6620): Optimization of Intra- and Intermolecular Polar Interactions of a New Ataxia Telangiectasia Mutated and Rad3-Related (ATR) Kinase Inhibitor. *J. Med. Chem.* **2019**, *62* (11), 5547–5561. https://doi.org/10.1021/acs.jmedchem.9b00426.

(32) Foote, K. M.; Nissink, J. W. M.; McGuire, T.; Turner, P.; Guichard, S.; Yates, J. W. T.; Lau, A.; Blades, K.; Heathcote, D.; Odedra, R.; Wilkinson, G.; Wilson, Z.; Wood, C. M.; Jewsbury, P. J. Discovery and Characterization of AZD6738, a Potent Inhibitor of Ataxia Telangiectasia Mutated and Rad3 Related (ATR) Kinase with Application as an Anticancer Agent. *J. Med. Chem.* **2018**, *61* (22), 9889–9907. https://doi.org/10.1021/acs.jmedchem.8b01187.

(33) Lücking, U.; Wortmann, L.; Wengner, A. M.; Lefranc, J.; Lienau, P.; Briem, H.; Siemeister, G.; Bömer, U.; Denner, K.; Schäfer, M.; Koppitz, M.; Eis, K.; Bartels, F.; Bader, B.; Bone, W.; Moosmayer, D.; Holton, S. J.; Eberspächer, U.; Grudzinska-Goebel, J.; Schatz, C.; Deeg, G.; Mumberg, D.; von Nussbaum, F. Damage Incorporated: Discovery of the Potent, Highly Selective, Orally Available ATR Inhibitor BAY 1895344 with Favorable Pharmacokinetic Properties and Promising Efficacy in Monotherapy and in Combination Treatments in Preclinical Tumor Models. *J. Med. Chem.* **2020**, *63* (13), 7293–7325. https://doi.org/10.1021/acs.jmedchem.0c00369.

(34) Zenke, F. T.; Zimmermann, A.; Dahmen, H.; Elenbaas, B.; Pollard, J.; Reaper, P.; Bagrodia, S.; Spilker, M. E.; Amendt, C.; Blaukat, A. Abstract 369: Antitumor Activity of M4344, a Potent and Selective ATR Inhibitor, in Monotherapy and Combination Therapy. In *Experimental and Molecular Therapeutics*; American Association for Cancer Research, 2019; pp 369–369. https://doi.org/10.1158/1538-7445.AM2019-369.

(35) Thomas, A.; Redon, C. E.; Sciuto, L.; Padiernos, E.; Ji, J.; Lee, M.-J.; Yuno, A.; Lee, S.; Zhang, Y.; Tran, L.; Yutzy, W.; Rajan, A.; Guha, U.; Chen, H.; Hassan, R.; Alewine, C. C.; Szabo, E.; Bates, S. E.; Kinders, R. J.; Steinberg, S. M.; Doroshow, J. H.; Aladjem, M. I.; Trepel, J. B.; Pommier, Y. Phase I Study of ATR Inhibitor M6620 in Combination With Topotecan in Patients With Advanced Solid Tumors. *JCO* **2018**, *36* (16), 1594–1602. https://doi.org/10.1200/JCO.2017.76.6915.

(36) Yap, T. A.; O'Carrigan, B.; Penney, M. S.; Lim, J. S.; Brown, J. S.; de Miguel Luken, M. J.; Tunariu, N.; Perez-Lopez, R.; Rodrigues, D. N.; Riisnaes, R.; Figueiredo, I.; Carreira, S.; Hare, B.; McDermott, K.; Khalique, S.; Williamson, C. T.; Natrajan, R.; Pettitt, S. J.; Lord, C. J.; Banerji, U.; Pollard, J.; Lopez, J.; de Bono, J. S. Phase I Trial of First-in-Class ATR Inhibitor M6620 (VX-970) as Monotherapy or in Combination With Carboplatin in Patients With Advanced Solid Tumors. *JCO* **2020**, *38* (27), 3195–3204. https://doi.org/10.1200/JCO.19.02404.

(37) Middleton, M. R.; Dean, E.; Evans, T. R. J.; Shapiro, G. I.; Pollard, J.; Hendriks, B. S.; Falk, M.; Diaz-Padilla, I.; Plummer, R. Phase 1 Study of the ATR Inhibitor Berzosertib (Formerly M6620, VX-970) Combined with Gemcitabine ± Cisplatin in Patients with Advanced Solid Tumours. *Br J Cancer* **2021**, *125* (4), 510–519. https://doi.org/10.1038/s41416-021-01405-x.

(38) Kim, R.; Kwon, M.; An, M.; Kim, S. T.; Smith, S. A.; Loembé, A. B.; Mortimer, P. G. S.; Armenia, J.; Lukashchuk, N.; Shah, N.; Dean, E.; Park, W.-Y.; Lee, J. Phase II Study of Ceralasertib (AZD6738) in Combination with Durvalumab in Patients with Advanced/Metastatic Melanoma Who Have Failed Prior Anti-PD-1 Therapy. *Annals of Oncology* **2022**, *33* (2), 193–203. https://doi.org/10.1016/j.annonc.2021.10.009.

(39) Dillon, M.; Guevara, J.; Mohammed, K.; Smith, S. A.; Dean, E.; McLellan, L.; Boylan, Z.; Spicer, J.; Forster, M. D.; Harrington, K. J. 450PD - A Phase I Study of ATR Inhibitor, AZD6738, as Monotherapy in Advanced Solid Tumours (PATRIOT Part A, B). *Annals of Oncology* **2019**, *30*, v165–v166. https://doi.org/10.1093/annonc/mdz244.012.

(40) Charrier, J.-D.; Durrant, S. J.; Golec, J. M. C.; Kay, D. P.; Knegtel, R. M. A.; MacCormick, S.; Mortimore, M.; O'Donnell, M. E.; Pinder, J. L.; Reaper, P. M.; Rutherford, A. P.; Wang, P. S. H.; Young, S. C.; Pollard, J. R. Discovery of Potent and Selective Inhibitors of Ataxia Telangiectasia Mutated and Rad3 Related (ATR) Protein Kinase as Potential Anticancer Agents. *J. Med. Chem.* **2011**, *54* (7), 2320–2330. https://doi.org/10.1021/jm101488z.

(41) Suzuki, A. Organoboron Compounds in New Synthetic Reactions. *Pure and Applied Chemistry* **1985**, *57* (12), 1749–1758. https://doi.org/10.1351/pac198557121749.

(42) Christ, H.-A.; Bourgat, Y.; Menzel, H. Optimization of Critical Parameters for Carbodiimide Mediated Production of Highly Modified Chitosan. *Polymers* **2021**, *13* (16), 2702. https://doi.org/10.3390/polym13162702.

(43) Nghiem, P.; Park, P. K.; Kim, Y.; Desai, B. N.; Schreiber, S. L. ATR Is Not Required for P53 Activation but Synergizes with P53 in the Replication Checkpoint *. *Journal of Biological Chemistry* **2002**, *277* (6), 4428–4434. https://doi.org/10.1074/jbc.M106113200.

(44) Kwok, M.; Davies, N.; Agathanggelou, A.; Smith, E.; Oldreive, C.; Petermann, E.; Stewart, G.; Brown, J.; Lau, A.; Pratt, G.; Parry, H.; Taylor, M.; Moss, P.; Hillmen, P.; Stankovic, T. ATR Inhibition Induces Synthetic Lethality and Overcomes Chemoresistance in TP53- or ATM-Defective Chronic Lymphocytic Leukemia Cells. *Blood* **2016**, *127* (5), 582–595. https://doi.org/10.1182/blood-2015-05-644872.

(45) Ghosh, S. Cisplatin: The First Metal Based Anticancer Drug. *Bioorganic Chemistry* **2019**, *88*, 102925. https://doi.org/10.1016/j.bioorg.2019.102925.

(46) Singh, N.; Miner, A.; Hennis, L.; Mittal, S. Mechanisms of Temozolomide Resistance in Glioblastoma - a Comprehensive Review. *Cancer Drug Resistance* **2021**, *4* (1), 17–43. https://doi.org/10.20517/cdr.2020.79.